

# **Synthesis and Characterisation of Polyphenol based Natural Deep Eutectic Solvents for Potential Recycling Applications**

**M.Sc. Thesis**

By

**RAHUL KUMAR SHARMA**



**DEPARTMENT OF CHEMISTRY  
INDIAN INSTITUTE OF TECHNOLOGY INDORE  
MAY, 2024**

# Synthesis and Characterisation of Polyphenol based Natural Deep Eutectic Solvents for Potential Recycling Applications

**A THESIS**

*Submitted in partial fulfillment of the  
requirements for the award of the degree  
of  
Master of Science*

*by*

**RAHUL KUMAR SHARMA**



**DEPARTMENT OF CHEMISTRY  
INDIAN INSTITUTE OF TECHNOLOGY INDORE  
MAY, 2024**

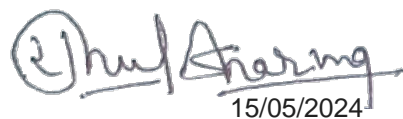


# INDIAN INSTITUTE OF TECHNOLOGY INDORE

## CANDIDATE'S DECLARATION

I hereby certify that the work which is being presented in the thesis entitled “**Synthesis and Characterisation of Polyphenol based Natural Deep Eutectic Solvents for potential Recycling Applications**” in the partial fulfillment of the requirements for the award of the degree of **MASTER OF SCIENCE** and submitted in the **DEPARTMENT OF CHEMISTRY, Indian Institute of Technology Indore**, is an authentic record of my own work carried out during the time period from July,2023 to May,2024 under the supervision of Dr. Tridib Kumar Sarma, Associate Professor, Department of Chemistry, IIT Indore.

The content presented in this thesis has not been submitted by me for the award of any other degree of this or any other institute.



15/05/2024

Signature of the Student with date  
(RAHUL KUMAR SHARMA)

-----

This is to certify that the above statement made by the candidate is correct to the best of my/our knowledge.



Signature of the Supervisor of M.Sc. thesis

(Dr. TRIDIB KUMAR SARMA)

-----

RAHUL KUMAR SHARMA has successfully given his M.Sc. Oral Examination held on **08.05.2024**.



Signature of Supervisor of MSc thesis  
Dr. Tridib Kumar Sarma  
Date: 15/05/2024

Convener, DPGC  
Dr. Umesh A. Kshirsagar  
Date:

## ACKNOWLEDGEMENT

First and foremost, I want to convey my sincere gratitude to Dr. Tridib Kumar Sarma, my supervisor, for his unwavering guidance and support throughout this project. Working under his supervision has proven to be immensely enriching and rewarding. I found great satisfaction in tackling various challenges and grasping the fundamental principles essential to my work. I am very thankful for his invaluable advice, suggestions, and encouragement towards my future academic pursuits.

I extend my gratitude to the faculty members of the Department of Chemistry, especially Prof. Biswarup Pathak and Dr. Debayan Sarkar as my PSPC Members, for their assistance across different facets of this endeavor.

I would like to thank all the staff members for their technical support. I am also thankful to the Sophisticated Instrumentation Centre (SIC), IIT Indore, and IIT Indore for providing the necessary infrastructure for conducting my research work.

And, I am profoundly grateful to my mentor, Mr. Suryakamal Sarma, whose continuous assistance across all aspects of this project was invaluable. My sincere gratitude is also extended to my lab mates, namely Ms. Amrita, Ms. Vidhi, Mr. Aditya, Mr. Tarun, Mr. Ravindra, Mr. Yonas and Ms. Aayushi for their assistance in both academic and non-academic affairs. I extend heartfelt thanks to all my batchmates and friends.

Finally, I express my profound love and gratitude to my beloved parents, Mr. Laxmikant Sharma and Mrs. Urmila Devi, for their unconditional love and support. I wish to convey my heartfelt regards to my dear brother, Mr. Puneet, Mr. Shakul and Mr. Gaurav. Also, I wish to convey my regards to my lovable sister, Ms. Kusum Sharma.



**Signature of the Student**

**(Rahul Kumar Sharma)**

**DEDICATION**

*Dedicated to  
My Family  
and  
Relatives.*

## **Abstract**

Natural deep eutectics solvents (NADESs) are being pursued actively for many biological as well as technological applications due to their higher thermal stability, solvation capacity and nontoxicity. Herein, we report a series of plant-based polyphenol derived deep eutectic solvents with high viscosity, thermal activity, and wide liquid temperature range. All the three NADESs are well studied by spectroscopic studies and established the possible bonding interactions between the hydrogen bonding species. Further, the application of DES as a green approach for the hydrometallurgical recycling process has been very well studied in recent years. However, the use of NADESs to leach the Li-ion battery cathode materials is rarely explored. We have proposed a green method for the leaching of valuable metals such as lithium, cobalt, manganese, and nickel from mixed spent Li-ion battery powders. Importantly, the mechanism of the leaching process has been further evaluated using spectroscopic techniques. We further highlight the prepared NADESs as an economical and environmentally friendly medium for metal recovery from spent LIBs.

## Table of contents

LIST OF FIGURES	VI
LIST OF REACTION SCHEME	VIII
LIST OF TABLES	VIII
ACRONYMS	IX
Chapter 1	
1. Introduction	
1.1. What are Deep eutectic solvents (DESs)?	1
1.2. Types and properties of Deep eutectic solvents	2
1.3. Applications of DESs	3
1.4. What are Natural deep eutectic solvents (NADES)?	5
Chapter 2	
2. Literature Overview	11
Chapter 3	
3. Experimental Section	
3.1. Materials	15
3.2. Spent Lithium-ion battery cathode extraction.	15
3.3. Instrumentation	16
3.4. Synthesis of NADESs	17
3.5. Dissolution of Lithium cobalt oxide (LiCoO <sub>2</sub> ) and leaching efficiency determination for prepared NADESs	19 21
3.6. Dissolution of Spent Lithium-ion batteries and leaching efficiency determination for prepared NADESs	
3.7. Recovery of dissolved metal ions from the NADESs	21
Chapter 4	
4. Result and Discussion	
4.1. Synthesis and Characterization of the prepared NADESs	24
4.2. UV-visible spectroscopy	24

4.3.	Fourier transformed IR (FTIR) Spectroscopy	26
4.4.	<sup>1</sup> H NMR Spectroscopy	29
4.5.	Physical properties of prepared NADESs	31
4.6.	Dissolution of metal ions into Prepared NADES	33
4.7.	Leaching Mechanism	37
4.8.	Metal Recovery from selective precipitation method	
Chapter 5		
5.	Conclusion	42
	Future Scopes	43
Chapter 6		
6.	References	44

## LIST OF FIGURES

**Figure 1.** A eutectic system of Component A and Component B.

**Figure 2.** Various properties of deep eutectic solvents.

**Figure 3.** Various applications of deep eutectic solvents.

**Figure 4.** Various properties and components of natural deep eutectic solvents.

**Figure 5.** Various properties and components of Polyphenols.

**Figure 6.** Structures of hydrogen bond donors and acceptor of naturally occurring polyphenols.

**Figure 7.** Recycling process for cathode of spent LIBs using NADES.

**Figure 8.** Various plant derived polyphenols based NADESs.

**Figure 9.** Recycling process for cathode of spent LIBs using ChCl:EG DES at different temperature scale.

**Figure 10.** Proposed mechanism for recycling process for cathode of spent LIBs using NADES.

**Figure 11.** Multistep selective chemical precipitation method.

**Figure 12.** UV-visible spectra of the prepared DESs with respect to their components.

**Figure 13.** FTIR spectra of TA-ChCl DES with respect to their components.

**Figure 14.** FTIR spectra of GA-ChCl DES with respect to their components.

**Figure 15.** FTIR spectra of Py-ChCl DES with respect to their components.

**Figure 16.** <sup>1</sup>H-NMR Spectrum of TA-ChCl DES.

**Figure 17.**  $^1\text{H}$ -NMR Spectrum of GA-ChCl DES.

**Figure 18.**  $^1\text{H}$ -NMR Spectrum of Py-ChCl DES.

**Figure 19.** Viscosity vs. shear rate plot and  $\ln \eta$  vs  $1/T$  plots correlated with Arrhenius Equation.

**Figure 20.** Leaching efficiencies of DESs towards Lithium cobalt oxide (LCO) powder at variable temperature scale.

**Figure 21.** Extraction of lithium and cobalt metal ions from LCO powder.

**Figure 22.** Extraction of valuable metals from spent LIB cathode.

**Figure 23.** SEM-EDX image of recovered Cobalt from LCO leachate.

**Figure 24.** SEM-EDX image of recovered Manganese and Nickel from spent LIB powder.

**Figure 25.** SEM-EDX image of recovered cobalt from spent LIB powder.

## LIST OF SCHEMES

**Scheme 1.** Synthesis of TA-ChCl DES.

**Scheme 2.** Synthesis of GA-ChCl DES.

**Scheme 3.** Synthesis of Py-ChCl DES.

## LIST OF TABLES

**Table 1.** Types of Deep Eutectic Solvents based on their components.

**Table 2.** Source of common polyphenols.

**Table 3.** Vibrational frequencies of TA-ChCl DES with respect to their components.

**Table 4.** Vibrational frequencies of GA-ChCl DES with respect to their components.

**Table 5.** Vibrational frequencies of Py-ChCl DES with respect to their components.

**Table 6.** Summary of NADESs prepared (physical features).

**Table 7.**  $E_a$  values as a function of temperature.

## ACRONYMS

<b>DESS</b>	Deep eutectic solvents
<b>HBDs</b>	Hydrogen-bond donors
<b>HBAs</b>	Hydrogen-bond acceptors
<b>NADESS</b>	Natural deep eutectic solvents
<b>THEDESS</b>	Therapeutic Deep eutectic solvents
<b>MP</b>	Melting point
<b>LIBs</b>	Lithium-ion batteries
<b>TA</b>	Tannic acid
<b>GA</b>	Gallic acid
<b>Py</b>	Pyrogallol
<b>ChCl</b>	Choline chloride
<b>NMR</b>	Nuclear magnetic resonance
<b>ICPAES</b>	Inductively coupled plasma atomic emission spectroscopy
<b>SEM</b>	Scanning electron microscopy
<b>EDS</b>	Energy dispersive spectroscopy
<b>FTIR</b>	Fourier transformed infrared



# 1. Chapter 1

## Introduction

### 1.1. What are deep eutectic solvents (DESSs)?

Eutectic solvents are a special category of solvents which are obtained by combining two or more components in specific proportions and the resulting mixture shows a lower melting temperature than that of individual components. The temperature, below which both the components of the eutectic solvent exist in solid form, is known as eutectic point. The depression in melting point of the bicomponent mixture attributed to that at a specific molar ratio, both component A and B shows eutectic behavior irrespective of the structure and reactivity of each component (Figure 1).<sup>1</sup>

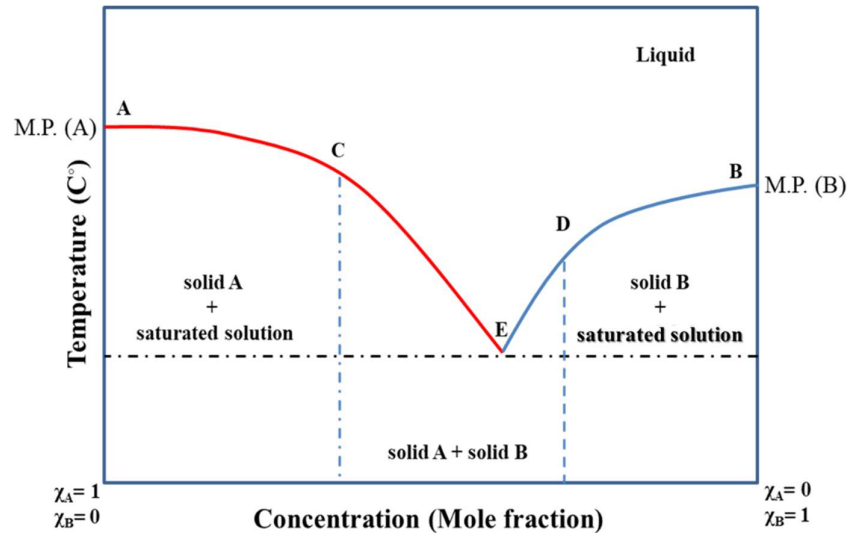


**Figure 1.** A eutectic system of component A and component B showing depression in melting point. Point A and B represents the melting point of Component A and Component B respectively. Point E represents the melting point and eutectic composition of the eutectic system. Points C and D show depressions in melting point at non-eutectic compositions.<sup>1</sup>

Some eutectic solvents show unexpectedly high depressions in their melting points. Such eutectic solvents are called deep eutectic solvents. The presence of hydrogen-bond donors (HBDs) and hydrogen-bond acceptors (HBAs) or Lewis/Bronsted acids and bases as the constituting unit of the DESs reveals the main cause for deep depression in melting points.<sup>1,2,5</sup> The complex hydrogen-bonding between HBAs and HBDs results in the depression of the melting point of the DESs.<sup>1</sup>

### 1.2. Types and properties of deep eutectic solvents

DESs can be classified majorly into 5 types:<sup>1</sup>

<b>Table 1:</b> Types of Deep Eutectic Solvents based on their components.	
<b>Type I</b>	consists of quaternary ammonium salt and a metal chloride
<b>Type II</b>	consists of a metal chloride hydrate and quaternary ammonium salt
<b>Type III</b>	formed by combining quaternary ammonium salt and hydrogen bond donors (an amide, carboxylic acid, polyphenols, or polyols)
<b>Type IV</b>	combining HBDs and metal chloride hydrate <sup>7</sup>
<b>Type V</b>	composed of non-ionic HBAs and HBDs <sup>8</sup>

DESs which are formed by combining natural products such as Choline halide (HBA), Urea, amino acids, sugars, organic acids, natural polyols etc. as potential hydrogen bond donors are called natural DESs (NADESs).<sup>2,6</sup> NADESs are biodegradable, biocompatible, have chemical renewability and reduced toxicity (Figure 2). DESs which contains active pharmaceutical ingredient as their components are called therapeutic DESs (THEDESs).<sup>2,5,6</sup>

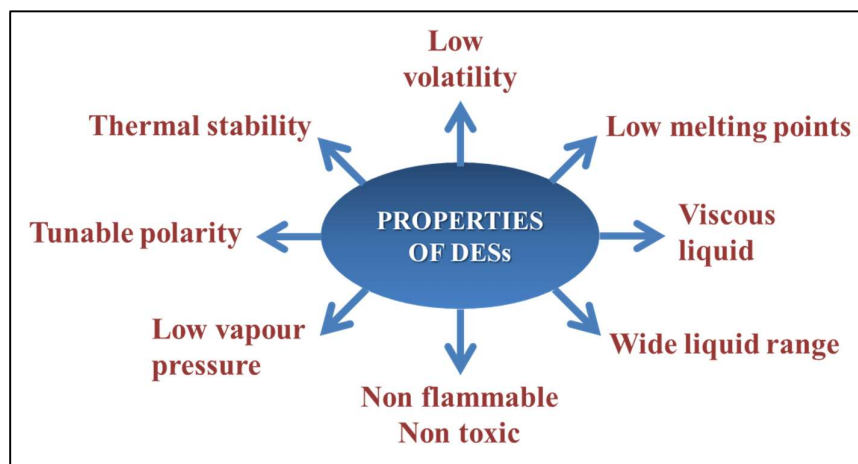


**Figure 2.** Various properties of deep eutectic solvents.

DESs are typically viscous, non-volatile, low toxic, low vapor pressure and can show high thermal stabilities, excellent solubility, fluidity, and conductivity. DESs turn opaque solid below its eutectic temperature. The properties of DESs are highly dependent on the nature of components.<sup>1</sup> This emerging class of solvents has numerous prospective applications in various research areas.

### 1.3. Applications of DESs

DESs can show widespread applications in various areas such as pharmaceuticals, metallurgy, battery technologies etc. (Figure 3). Tremendous research is on the way to explore the potential applications of DESs.<sup>1</sup> Some of the applications of DESs that have been explored are included in this section:

#### 1.3.1. Metallurgic applications

Deep eutectic solvents (DESs) demonstrate considerable potential for the extraction and recycling of metals in solution, ore refining and electrodeposition due to the notable high solubilities and electrical conductivities exhibited by metals and metal salts in these solvents.<sup>1,10,11,12,13</sup> In the early 2000s, Abbott *et al.* conducted a series of initial investigations on deep eutectic solvents (DESs). Their studies focused on the electroplating applications of DESs, showcasing their considerable potential.<sup>14,15</sup> The positive outcomes of these studies have

spurred the interest of numerous research groups, and motivated for exploration and examination of these innovative materials.

### **1.3.2. Batteries and Power systems**

Rechargeable batteries are widely used in laptops, mobiles, and electric vehicles. The demand for rechargeable batteries has increased in the era of fast urbanization and electrification. The electrolytes currently used in the batteries resulted in several batteries failures.<sup>1</sup> DESs are considered as a potential substitute for the electrolytes in rechargeable batteries due to their wide liquid range, high thermal stabilities, and electrical conductivities, etc.<sup>1</sup>

### **1.3.3. Biocatalysis**

Biocatalysis refers to the use of natural catalysts, such as enzymes and microorganisms, to facilitate and accelerate chemical reactions. Biocatalysis plays a crucial role in the synthesis of pharmaceuticals, fine chemicals, and other products, contributing to the development of sustainable and efficient methods in the field of chemistry. Generally, Biocatalysis is usually conducted in aqueous solution. Therefore, the meticulous selection of both the enzyme and the solvent is crucial to produce valuable end products. DESs constitutes of amino acids, sugars, and vitamins, etc. which can support varieties of enzymes and substrates. Thus, DESs can be a potential candidate to facilitate biocatalytic reactions.<sup>16,17,18</sup>

### **1.3.4. Biomass processing**

Biomass refers to organic materials derived from living or dead organisms, primarily plants and microorganisms. Biomass includes a wide range of biological materials such as wood, crop residues, animal waste and algae, etc. Biomass is a renewable and sustainable source of energy and feedstock for various applications. The conversion of this plentiful and inexpensive biomass into useful products such as biofuel or energy is called biomass processing. Many reaction pathways involved in the pretreatment of biomass are found to be toxic,

unscalable, and expensive processes.<sup>19,20</sup> Deep eutectic solvents (DESs) exhibit noteworthy potential to address this issue. They possess multifunctionality, specifically in the domains of solubilization, extraction, and the subsequent generation of value-added products from lignocellulosic material.<sup>21,22,23,24,25</sup>

### 1.3.5. Medicine

Researchers are looking for new ways to deliver drugs to the targeted areas. Many pharmaceutical compounds are found to form DESs. Thus, DESs could serve as drug solubilization vehicles.<sup>26-28</sup> Morrison et al. demonstrated that deep eutectic systems comprising reline and malonic acid-choline chloride exhibited solubility levels for various solutes, such as benzoic acid, danazol, itraconazole, and griseofulvin, up to 22,000 times greater than that of water.<sup>26</sup>

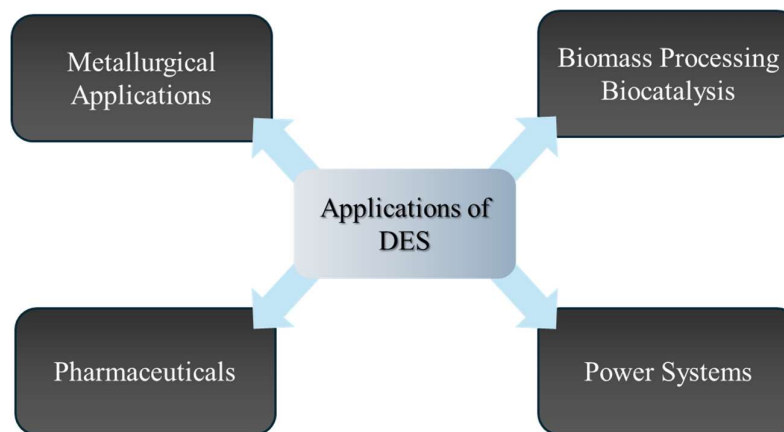


**Figure 3.** Various applications of deep eutectic solvents.<sup>1</sup>

### 1.4. What are natural deep eutectic solvents (NADESs)?

Natural deep eutectic solvents (NADESs) are a subclass of deep eutectic solvents that are derived from natural resources. These solvents are composed of naturally occurring compounds, such as organic acids (e.g., citric acid, malic acid), sugars, polyphenols, and natural bases (e.g., choline, amino acids). NADESs are biodegradable, biocompatible, have chemical renewability and reduced toxicity

(Figure 4). DESs which contains active pharmaceutical ingredient as their components are called therapeutic DESs (THEDESs).<sup>2,5,6</sup> These bioactive molecules are bio-accessible, biocompatible and show valuable properties as non-toxic, antioxidants, anti-inflammatory, anticancer, and antibacterials and anti-obesity etc.<sup>31</sup>

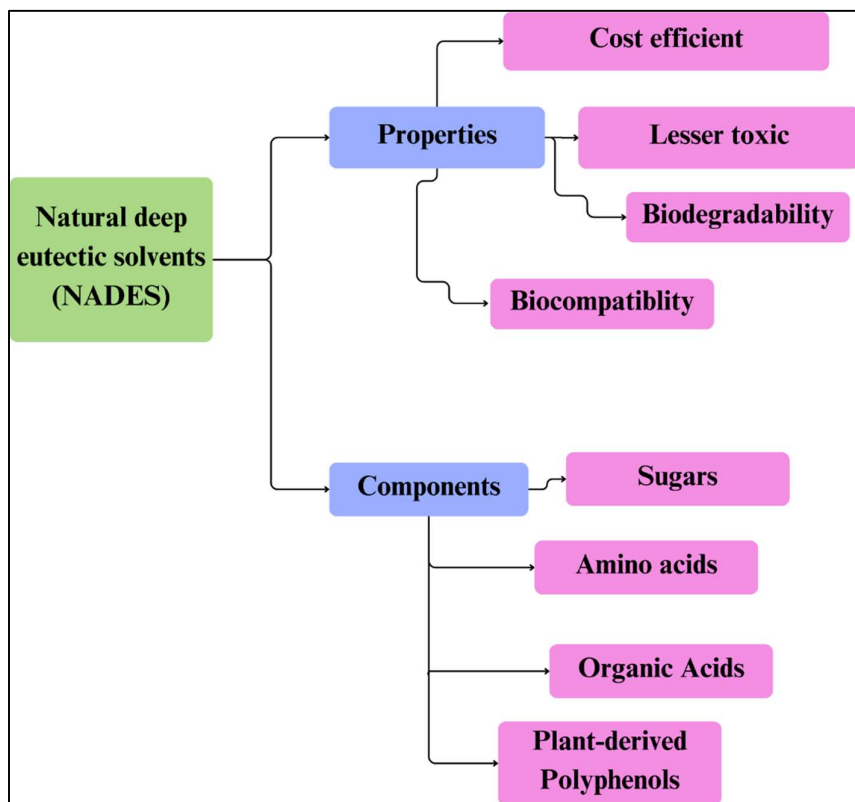


**Figure 4.** Various properties and components of natural deep eutectic solvents.

Vegetables and fruits are rich in polyphenols, phenolics and flavones. These polyphenols, due to the presence of multiple non-covalent bonding sites, can serve as a potential hydrogen bond donor (HBD) for deep eutectic systems. Polyphenols are naturally obtained from fruits, vegetables, nuts, mushrooms etc. and are also synthesized chemically. Among them, anthocyanins, catechins, flavones, phenolic acids, tannic acid, gallic acid, pyrogallol, and caffeic acid are some of the examples of naturally extracted polyphenols (Figure 5).<sup>31</sup>

Choline (Figure 6), a non-toxic, inexpensive quaternary ammonium cation, is typically used as a supplement in animal feed and is commonly used as a component (HBA) in most of the DESs reported to date.<sup>2,9</sup>

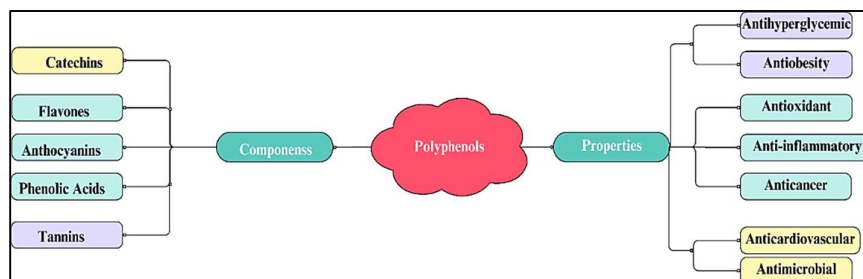


**Figure 5.** Various properties and components of Polyphenols.

<b>Table 2: Source of common polyphenols.</b>	
<b>Name</b>	<b>Common source</b>
Tannic acid	Oak
Gallic acid	Tea leaves
Pyrogallol	Eurasian watermilfoil
Caffeic acid	Coffee bean
Ellagic acid	Oak
L-Dopa	Velvet beans

Plant-derived polyphenols-based NADES (Table 2) are found to exhibit a wide liquid range and high thermal stability above 150 °C.<sup>3</sup> It is noteworthy that polyphenols are serving as potential therapeutic agents, antioxidants, adhesives, and redox-active compounds. Therefore, Plant-derived polyphenols-based NADES are of supreme importance and can exhibit many unexplored applications.

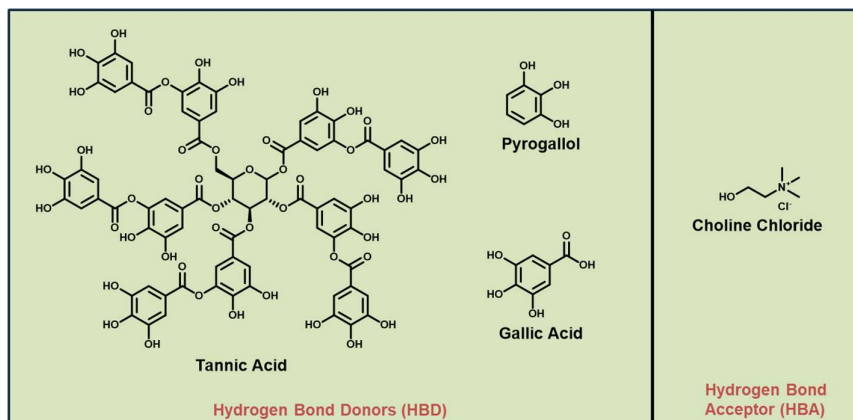


**Figure 6.** Structures of hydrogen bond donors and acceptor of naturally occurring polyphenol based natural deep eutectic solvents (NADES).<sup>3</sup>

The journey of digitalization and development of a country results in increased energy consumption and requires a good source of energy to fulfil the overloading requirements. Electrification is one of the best solutions sought for increased energy consumption because no pollutants are emitted as by-products. The electrification of automobiles to avoid the emission of greenhouse gases requires Li-ion batteries. Lithium-ion batteries (LIBs) are popularly used in laptops, mobiles and electric automobiles which also leads to piles of LIB waste. Lithium-ion batteries contain valuable materials such as lithium cobalt oxide, lithium nickel manganese oxide as their cathode component, aluminum foil, electrolytes and polyvinylidene fluoride binder etc. LIBs contain 15 weight% of cathodes as Cobalt. Cobalt, accumulated in large amounts, is an environmental and health concern. Thus, Safe disposal of spent LIB waste and supply of the raw materials for the manufacturing of the Li-ion batteries is a challenging task.<sup>4</sup> Maximizing the use of metal elements limits the risks of material shortages and reduces the dependency on supply chains. The recycling of these components from spent LIBs can minimize the impact of spent LIB waste on human health and the natural environment and will also

lead in relieving the stress from the supply chain of raw materials required for batteries production.<sup>4</sup>

At present, the common methodologies involved in the recycling of valuable elements in cathode of lithium-ion batteries includes pyrometallurgy, bio-metallurgy and hydrometallurgy etc. Pyrometallurgy uses high operating temperatures (>1400 °C), high energy consumptions and harmful off-gas emissions. Thus, high safety and precautionary measures involved in pyrometallurgy. On the other hand, recycling of cathode of spent LIBs using hydrometallurgy exhibits high leaching rate and lower energy cost than that of pyrometallurgy but involves large amount of harmful chemicals (caustic agents) and long processing times which makes it inconvenient to environment and involved workers. To overcome drawbacks of the above methodologies, new methodologies for recycling of e-waste still needed to be developed.<sup>31</sup>

Nowadays, DESs are emerging as a popular class of leaching agent for the extraction of valuable metals such as lithium, cobalt, nickel, and manganese present in spent lithium-ion batteries due to their high affinity towards metal oxides and their salts. This method requires lower temperature than pyrometallurgy and no additional solvent extractants are required in the process. Petrochemicals based molecules have been used as the components in DESs used for recycling process, so far. NADESs are potential candidates for extraction and recycling of metals from e-waste which also reduces the dependency on petrochemicals. Hence, NADESs based recycling method is a greener method for extraction of valuables from e-waste. The standard recycling of LIBs (Figure 7) using NADES commences with the disassembly of the lithium-ion battery (LIB), followed by immersing the cathode in a deep eutectic solvent (DES). After heating and agitation, the resultant leachate undergoes filtration, enabling the separation of residual conductive carbon. Through precipitation, the

dissolved metal ions, including lithium or cobalt, can be reclaimed for utilization in alternative energy applications.<sup>31</sup>

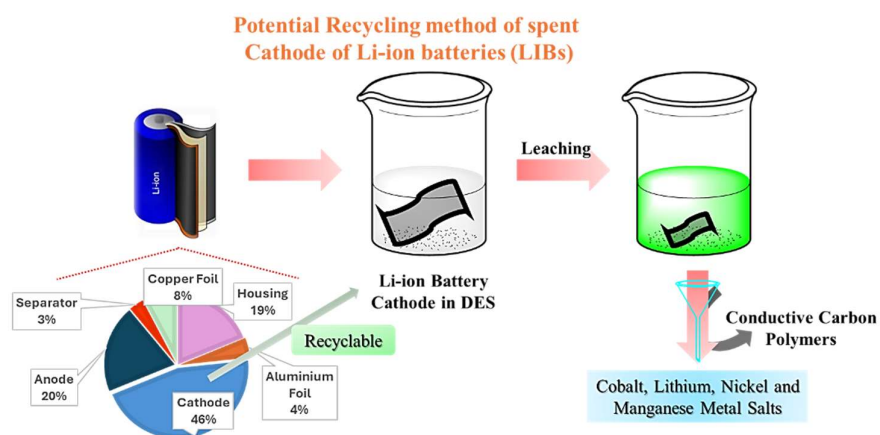


**Figure 7.** Recycling process for cathode of spent LIBs using NADES.<sup>31</sup>

## 2. Chapter 2

### Literature Overview

Deep eutectic solvents are the solvents which are formed by mixing hydrogen-bond acceptors and hydrogen-bond donors in a specific proportion. These solvents exhibit high thermal stability, low melting point and non-toxic to health, biodegradable and ecofriendly. Thus, DESs can find potential applications in diverse research areas. In 2003, Abbott *et al.* reported an unusual depression in melting at the eutectic composition, (2:1) of urea (HBD,  $T_m \approx 133$  °C) and choline chloride (HBA,  $T_m \approx 302$  °C) respectively resulted in a liquid showing melting point at 12 °C. Using symmetry and functional group as factors for DES synthesis, this group reported numerous DESs. Among all these DESs, ChCl-Urea DES exhibit the lowest melting point ( $T_m \approx 12$  °C). Abbott *et al.* named this mixture as “deep eutectic mixture or solvent”. This obvious depression in melting point was attributed to possible hydrogen bonding between choline chloride and urea.<sup>33</sup>

In 2004, Abbott *et al.* demonstrated that deep eutectic solvents (DES) can be synthesized through the interaction of choline chloride and carboxylic acids (monocarboxylic acid, dicarboxylic acid, and tricarboxylic acid). The diverse properties of these solvents are notably influenced by the structural features of the carboxylic acid component. DES found to be efficient to solubilize metal oxides and metal salts, suggesting potential applications in metal extraction processes.<sup>10</sup>

Some deep eutectic solvents constitute of naturally occurring sugars, biomolecules, and amino acids as HBDs and choline chloride as HBAs. Such DESs are called natural deep eutectic solvents which are biodegradable, biocompatible, and non-hazardous to health. Matías L. Picchio *et al.* in 2022, synthesized a series naturally occurring plant derived polyphenols-based NADES using choline chloride as hydrogen-bond acceptor (Figure 8). The group demonstrated the ability of vanillyl alcohol-based NADES to behave like bio-adhesives in

combination with gelatin. Also, tannic acid-based NADES exhibits the properties of corrosion protector of mild steel when combined with an acrylic layer.<sup>3</sup>

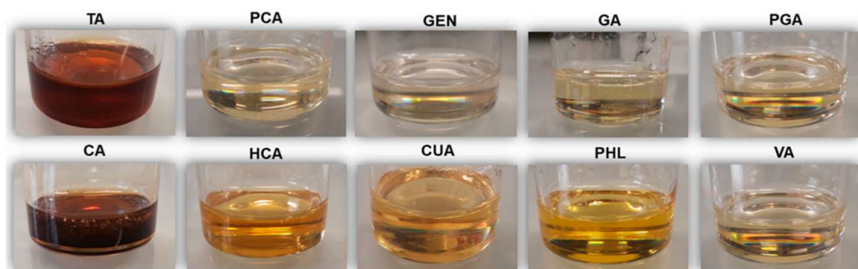


**Figure 8:** Various plant derived polyphenols based NADES.<sup>3</sup>

In 2019, Ganguli Babu *et al.* reported an exciting technology to recycle valuable elements from spent LIBs effectively using ethylene glycol-based DES where choline chloride was used as hydrogen-bond acceptor (Figure 9). This technology minimizes the usage of harmful chemicals and high temperatures for the purpose of recycling e-waste. This method shows leaching efficiency of 99.3% at 180 °C.<sup>32</sup>

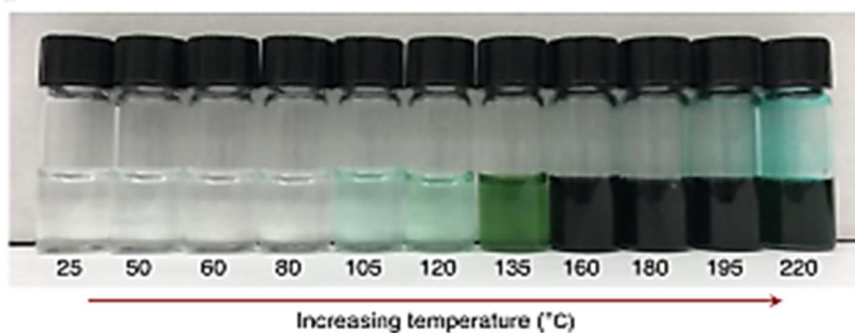


**Figure 9.** Recycling process for cathode of spent LIBs using ChCl:EG DES at different temperature scale.<sup>32</sup>

In 2021, Yanhong Chao *et al.* outlined a leaching method to recycle spent LIBs for recovery of valuable metals (lithium, cobalt, and manganese) using mixture of deep eutectic solvent and organic acids. Leaching efficiency for this method was reported to be 99% from LIB waste (Figure 10).<sup>34</sup>

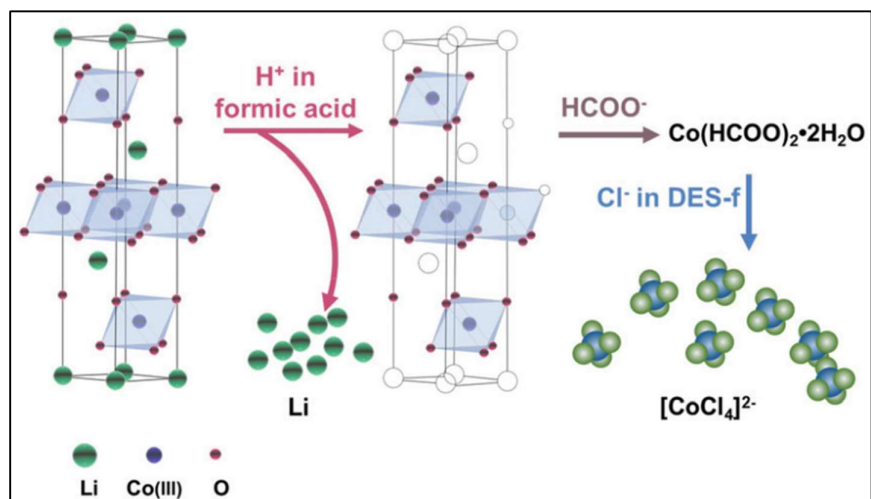


**Figure 10.** Proposed mechanism for recycling process for cathode of spent LIBs using NADES.<sup>34</sup>

Qi Meng et al. proposed a novel multistep directional precipitation method for extraction of beneficial metals from the end-of life batteries (Figure 11). The group used sodium hydroxide and sulphuric acid in 3 vol% H<sub>2</sub>O<sub>2</sub> solution as a leaching agent followed by multistep directional precipitation method for extraction of metals such as lithium, cobalt, manganese and nickel from spent batteries at different pH and respective reaction conditions<sup>37</sup>.

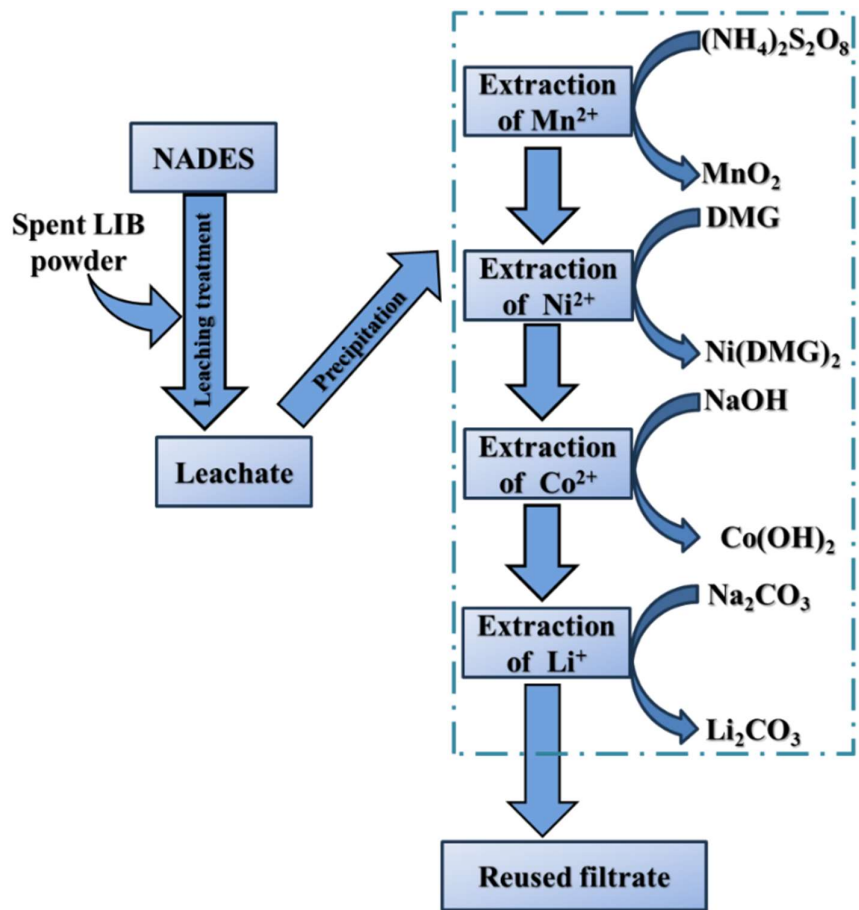


**Figure 11.** Multistep selective chemical precipitation method.

### **3. Chapter 3**

#### **Experimental Section**

In this report, we are mainly working on the synthesis of natural polyphenols (pyrogallol, gallic acid and tannic acid) hydrogen bond donor-based **Type III** binary DES using Choline chloride as hydrogen bond acceptor for their potential recycling applications.

#### **3.1. Materials**

Choline chloride was purchased from Avra, India. Tannic acid, gallic acid and pyrogallol were purchased from Sigma-Aldrich. HPLC water purchased from SRL, India was used throughout the experiments. Lithium cobalt oxide (LCO) was purchased from TCI India. Durapore membrane filter of 0.2  $\mu\text{m}$  pore size was purchased from Axiva. Ammonium persulfate, dimethylglyoxime, sodium carbonate, sodium hydroxide and hydrochloric acid were purchased from SRL, India. All the chemicals were used without further purification.

#### **3.2. Spent Lithium-ion battery cathode extraction**

A variety of end-of-life lithium-ion batteries from sources like laptops and mobile phones were collected from scrap markets. In these batteries, the cathode consisted of a mix of active materials applied to both sides of an aluminum foil (Al). Generally, the active material contained 80 - 85% metal oxide powder, 10% polyvinylidene fluoride (PVDF), and 5% black acetylene. Initially, the cathodes were crushed with a metal crusher, then heated at 700  $^{\circ}\text{C}$  for 2 hours to remove the PVDF. Following this, the treated foils were ground in a ball mill for 20 minutes. The final product was sieved with a 100  $\mu\text{m}$  mesh to separate aluminum fragments from the active material.

### **3.3. Instrumentation**

#### **UV-visible Spectroscopy**

The physical and chemical interactions among the components of NADES were monitored by UV-visible in a PerkinElmer Lambda 750 UV Spectrometer at  $10^{-4}$  mM concentration of all the components of NADES and NADESs. To understand the leaching mechanism, UV-visible spectroscopy was used with a setup where Deep Eutectic Solvents (DESs) were sandwiched between quartz plates for analysis.

#### **Fourier transformed IR (FTIR) Spectroscopy**

The physical and chemical interactions among the components of NADES were monitored by FTIR spectroscopy using a Bruker Alpha II instrument in the range of  $500\text{-}4000\text{ cm}^{-1}$  with resolution of employing an ATR module with a diamond window.

#### **NMR Spectroscopy**

$^1\text{H}$  nuclear magnetic resonance (NMR) spectrum for all three NADESs were recorded in a Bruker Avance NEO 500 ascend Bruker BioSpin international AG equipment with TMS as the standard using deuterated dimethyl sulfoxide ( $\text{DMSO-d}_6$ ) as solvent at room temperature.

#### **Rheological measurements**

Rheological tests were carried out on a rheometer using a PP25 mm cone-plate geometry of 25 mm radius with a gap of 0.5 mm. The viscosity vs. shear rate measurements for Tannic acid and pyrogallol based NADESs were recorded from  $0.1\text{ s}^{-1}$  to  $1000\text{ s}^{-1}$  at  $25\text{ }^\circ\text{C}$  at a constant strain of 1 %. The viscosity vs. shear rate measurements for Gallic acid-based NADES could not be measured because of its crystallinity point at  $35\text{ }^\circ\text{C}$ . The logarithmic value of Viscosity is plotted with shear rate. To measure temperature-dependent viscosity, the deep eutectic solvents (DESs) were positioned in a parallel plate geometry, and the temperature was varied from  $2\text{ }^\circ\text{C}$  to  $80\text{ }^\circ\text{C}$ .

The natural logarithmic values of viscosity were plotted against  $(1/T)$  ( $K^{-1}$ ) correlated with Arrhenius equation.

### **ICPAES Measurements**

The metal concentrations in the leaching solutions were determined using an Inductively Coupled Plasma Atomic Emission Spectrometer (ICPAES) (ARCOS, Spectro-Analytical Instruments, Germany). The leachate samples were diluted with 2%  $HNO_3$  solution prior to analysis. Similarly, to determine metal concentrations in the solid samples of lithium cobalt oxide (LCO) and spent lithium-ion battery (LIB) powders, the solid samples were processed with a microwave digester (Anton Paar Microwave Go) at 150 °C for 15 minutes in a solution containing 3 ml of HCl, 1 ml of  $HNO_3$ , and 2 ml of HF acids. After microwave digestion, the samples were diluted with HPLC-grade water for analysis.

### **Scanning Electron Microscopy**

The morphological behavior and Energy Dispersive X-ray (EDX) microanalysis of the recovered metal compounds were analyzed using a Carl-Zeiss Supra 55 Field Emission scanning electron microscope (FE-SEM) with a gold coating on the thoroughly dried samples.

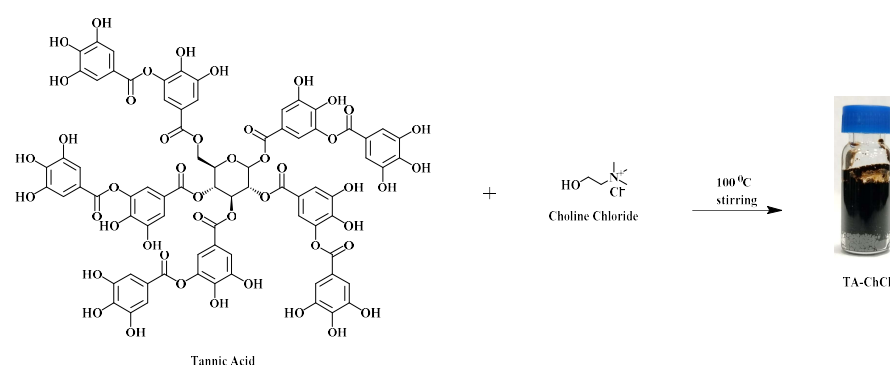
## **3.4. Synthesis of NADESs**

Plant-derived polyphenol-based NADESs were prepared using the common method of heating and stirring. Initially, the hydrogen bond donors and hydrogen bond acceptors for the NADESs were combined and heated at high temperatures with continuous stirring to create a homogeneous liquid, known as HBD-ChCl.

### **3.4.1. Synthesis of Tannic acid-ChCl NADES (TA-ChCl DES)**

The NADES containing tannic acid (as the hydrogen bond donor) and choline chloride (as the hydrogen bond acceptor) was synthesized using a simple heating and stirring method, as illustrated in [Scheme 1](#).

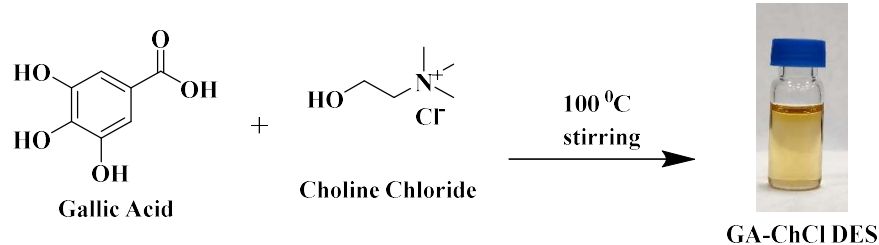
A 50 mL round-bottom flask was used, into which choline chloride and tannic acid were added in a molar ratio of 20:1. Specifically, 1.39 grams of choline chloride were taken, followed by the addition of 850 milligrams of tannic acid to the flask. The reaction mixture was then stirred at 100 °C for 12 hours, resulting in a homogeneous, viscous, translucent brownish liquid identified as TA-ChCl DES.



**Scheme 1.** Synthesis of TA-ChCl DES.

### 3.4.2. Synthesis of Gallic acid-ChCl NADES (GA-ChCl DES)

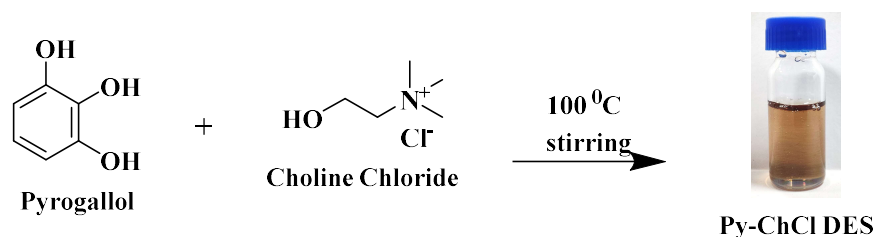
The gallic acid-based NADES was synthesized using the same heating and stirring method, as depicted in [Scheme 2](#). A 50 mL round-bottom flask was used to combine choline chloride (HBA) and gallic acid (HBD) in a molar ratio of 3:1. Specifically, 3.125 grams of choline chloride were taken to which 1.41 grams of gallic acid were added. The reaction mixture was stirred at 100 °C for 12 hours to obtain a homogeneous viscous yellowish liquid termed GA-ChCl DES.



**Scheme 2.** Synthesis of GA-ChCl DES.

### 3.4.3. Synthesis of Pyrogallol-ChCl NADES (Py-ChCl DES)

The pyrogallol-based NADES was synthesized by using the same method (Scheme 3). In a 50 mL round bottom flask, choline chloride (HBA) and pyrogallol (HBD) are taken in molar proportion of 2:1, specifically 1.39 g of Choline chloride and 630 mg of pyrogallol was mixed and stirred at 80 °C for 12 hours. A homogeneous brownish transparent solution was obtained termed Py-ChCl DES.



**Scheme 3.** Synthesis of Py-ChCl DES.

### 3.5. Dissolution of Lithium cobalt oxide (LiCoO<sub>2</sub>) and leaching efficiency determination for prepared NADESs

Lithium cobalt oxide (LiCoO<sub>2</sub>) powder is a key active material in the cathodes of lithium-ion batteries. Leaching experiments were conducted with three different NADESs, using LiCoO<sub>2</sub> as a model compound, to examine their efficiency in extracting lithium and cobalt. To calculate the leaching efficiency for these experiments, a specific formula was employed, as detailed below:

$$\text{Leaching efficiency} = \frac{CV}{M} \times 100$$

where,  $C$  represents the final concentration of metal(mg/L),  $V$  is the volume of initial leaching solution(L), and  $M$  is the mass of the initial amount of metal ions (Li, Co, Mn and Ni) in the substrate.

### **3.5.1. Time-dependent leaching of LCO using prepared NADESs**

The solubility of lithium cobalt oxide (LCO) in the prepared NADESs was quantitatively determined using a method described by Babu et al. For the metal extraction experiments, LCO powder (50 mg) was mixed with the prepared NADESs (2.5 g) in separate round-bottom flasks. The mixtures were stirred at 140 °C for up to 24 hours. Small aliquots (50mg) were taken from the reaction mixture at 1, 2, 4, 8, 12, 18, and 24-hour intervals to assess the change in leaching efficiency over time.

After collection, the samples were diluted with aqueous HNO<sub>3</sub>. The leachates, containing metal ions from the NADES, were then filtered through 0.2 μm nylon syringe filters to remove any unreacted LCO powder. The filtrates were analyzed using inductively coupled plasma atomic emission spectroscopy (ICPAES) to determine the concentrations of lithium and cobalt metal ions in the solution.

### **3.5.2. Temperature-dependent leaching of LCO using prepared NADESs**

The optimal temperature for metal extraction was identified through a series of leaching experiments. In these experiments, lithium cobalt oxide (LCO) powder (20 mg) was mixed with prepared NADESs (1 g) in separate round-bottom flasks. The reaction mixtures were stirred at various temperatures, ranging from 80 °C to 160 °C, for 24 hours. After leaching, the NADESs were diluted with 2% aqueous HNO<sub>3</sub> and thoroughly sonicated. The dissolved metal ion rich NADESs were filtered through 0.2 μm nylon syringe filters to remove any unreacted LCO powder. The concentrations of metal ions in the resulting leachates were then determined using inductively coupled plasma atomic emission spectroscopy (ICPAES).

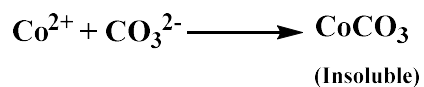
### **3.6. Dissolution of Spent Lithium-ion batteries and leaching efficiency determination for prepared NADESs**

To extend the leaching experiments conducted with lithium cobalt oxide (LCO) powder to spent lithium-ion batteries, these batteries were mechanically disassembled, crushed, and calcinated to create spent battery powder for effective dissolution in leaching agents. In the extended leaching experiments, 50 mg of spent battery powder was mixed with 2.5 g of prepared NADESs in three separate round-bottom flasks. The mixtures were stirred at 140 °C for up to 24 hours. Samples of 50 µL were extracted from the reaction mixtures at 1, 2, 4, 8, 12, 18, and 24-hour intervals to monitor the effect of time on leaching efficiency. After dilution with 2% aqueous HNO<sub>3</sub>, the leachates were filtered through 0.2 µm nylon syringe filters to separate unreacted battery components. The concentrations of lithium, cobalt, manganese, and nickel ions in the filtrates were determined using inductively coupled plasma atomic emission spectroscopy (ICPAES).

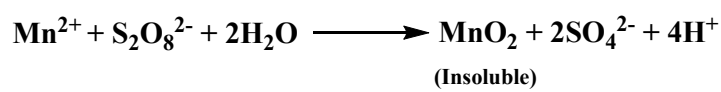
### **3.7. Recovery of dissolved metal ions from the NADESs**

Metal ions dissolved in the leachate from treated lithium cobalt oxide (LCO) were recovered through a simple chemical precipitation method.<sup>32</sup> In the case of leachate from spent lithium-ion batteries (LIB), the metal ions were converted into insoluble precipitates using a multi-stage directional chemical precipitation method.<sup>37</sup> This involved adding appropriate chemical precipitants to transform the soluble metal ions in the NADES into sparingly soluble or insoluble compounds, facilitating their recovery.

In the case of LCO leachate, the soluble Co<sup>2+</sup> metal ions were precipitated out in form of insoluble black colored CoCO<sub>3</sub> precipitate due to its low solubility in water by treating the leachate with saturated sodium carbonate solution. The precipitation reaction can be summarized as:



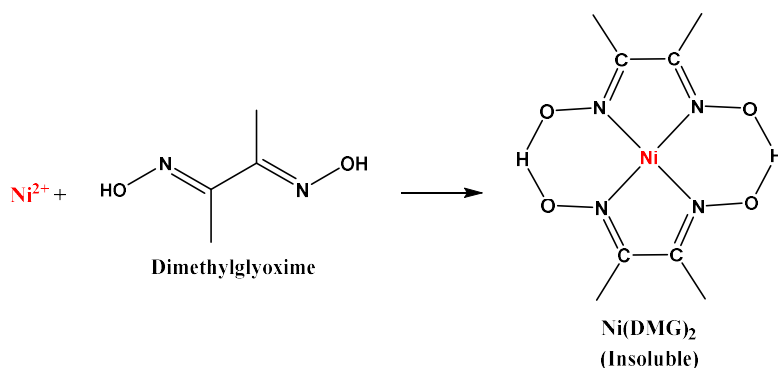
For LIB leachate, the soluble metal ions were precipitated using selective precipitation method as followed by Qi meng *et al.* The multistage precipitation begins with the precipitation of  $\text{Mn}^{2+}$  ions. The leachate was treated with aqueous ammonium persulphate solution (3 times more concentrated than the concentration of  $\text{Mn}^{2+}$  ions) at  $90^\circ\text{C}$  for 2 hours resulting into a mixture of  $\text{MnO}_2$  and  $\text{Mn}_2\text{O}_3$ . The precipitation reaction can be given as:



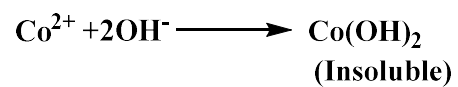
and,



The resultant precipitate was filtered out using cellulose filter paper and the left filtrate was treated with alcoholic solution of dimethylglyoxime for 30 min to separate out nickel in form of a water insoluble cherry red colored compound,  $\text{Ni}(\text{DMG})_2$ . The precipitation can be written as:



The precipitate was filtered out and resultant filtrate was further treated with  $\text{NaOH}$  to obtain cobalt metal ions into insoluble  $\text{Co}(\text{OH})_2$ . The precipitation reaction goes as per the equation given below:



All the recovered metal precipitates were washed with deionized water and methanol and dried at 55°C. All the precipitates were analyzed using morphological analysis and Energy-Dispersive X-ray (EDX) microanalysis to obtain more detailed information about their composition.

## 4. Chapter 4

### Result and Discussion

#### 4.1. Synthesis and Characterization of the prepared NADESs

Herein, Type III binary deep eutectic solvents (DESs) were synthesized using the heating and stirring method, with choline chloride serving as the hydrogen bond acceptor and plant-derived polyphenols such as tannic acid, gallic acid, and pyrogallol acting as hydrogen bond donors. A homogeneous liquid was obtained after 12 hours of heating and stirring.

The DESs made with tannic acid and pyrogallol were deep brown viscous liquids at room temperature, while the DES made with gallic acid was a transparent, low-viscosity yellowish liquid above 40 °C, which solidified below 35 °C. Various natural Deep Eutectic Solvents (NADESs) based on Choline chloride and organic acids are at risk of degradation due to the possibility of an esterification reaction occurring between the carboxylic groups and the alcohol moiety of the choline chloride.

Consequently, the purities and stabilities of all three NADES were assessed using proton nuclear magnetic resonance (NMR) spectroscopy, UV-visible spectroscopy, and Fourier transformed Infrared (FTIR) spectroscopy.

#### 4.2. UV-visible spectroscopy

UV-visible spectra for all three DES were recorded at  $10^{-4}$  mM concentration. From the UV-visible spectrum of tannic acid, choline chloride and TA-ChCl DES (Figure 12a), it is observed that the peak at 276 nm and 213 nm of tannic acid remains unshifted in the case of DES with slight increase in intensity. The peak value at 276 nm and 213 nm in the UV spectrum shows that tannic acid has not undergone

any structural changes and is intact in DES. This shift in the intensity of TA-ChCl DES is attributed to possible hydrogen-bonding due to the presence of HBA and HBD as DES constituents.

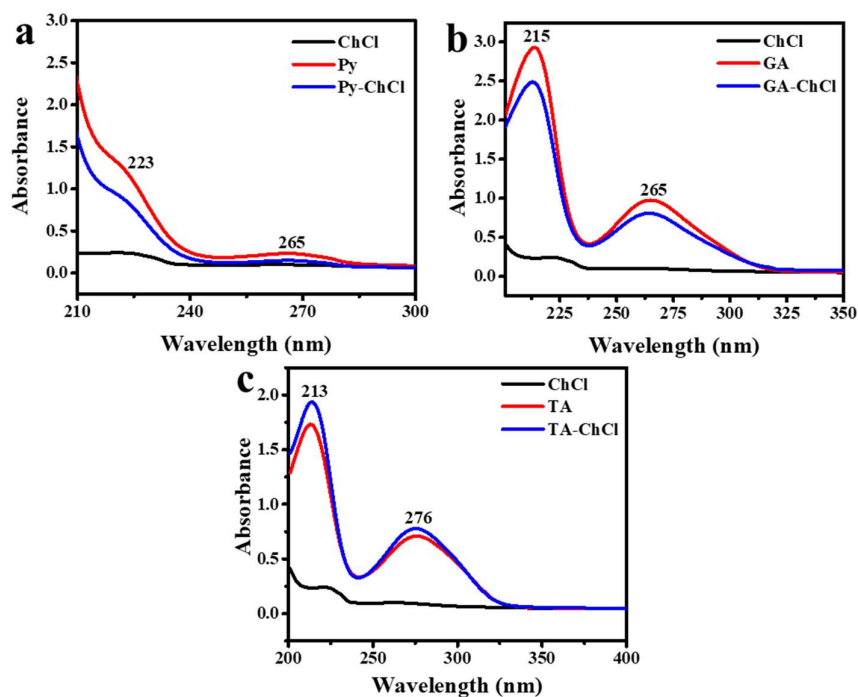


**Figure 12.** UV-visible spectra of the prepared DESs with respect to their components. **a.** TA-ChCl DES, **b.** GA-ChCl DES and **c.** Py-ChCl DES.

Following the trend, in the case of gallic acid and pyrogallol based DES (Figure 12b, c), the peaks of corresponding polyphenols remain intact with minimal decrease in intensity. This suggests that the properties of the individual polyphenols as well as choline chloride in the DES form remains unchanged and only non-covalent weak interactions are taking place. As hydrogen bond donor-acceptor components are involved in the DES formation, hydrogen bonding interactions are most likely to happen.

### 4.3. Fourier transformed IR (FTIR) Spectroscopy

The interactions playing role in the formation of NADESs were analyzed using IR spectroscopy. No emergence of new stretching frequencies in the spectrum of prepared NADESs and minor shifts in the stretching frequencies of the potential hydrogen-bonding sites present in their components confirms non-covalent interactions such as hydrogen-bonding among their components playing a crucial role in the formation of natural deep eutectic solvents. These non-covalent interactions between choline chloride and three different HBDs are evident from FTIR spectra of all three NADESs and its components.

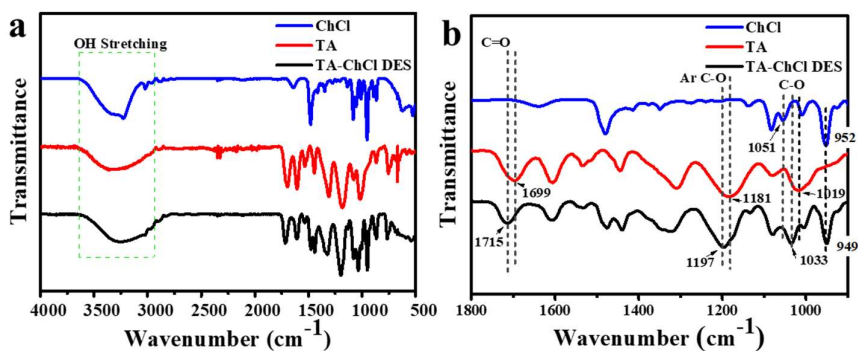


**Figure 13.** a. FTIR spectra of TA-ChCl DES with respect to their components and b. extended FTIR spectra to 1800-600  $\text{cm}^{-1}$  range.

<b>Table 3.</b> Vibrational frequencies of TA-ChCl DES with respect to their components.			
<b>Tannic Acid</b>	<b>Choline Chloride</b>	<b>TA-ChCl DES</b>	<b>Mode</b>
1699 $\text{cm}^{-1}$	-	1715 $\text{cm}^{-1}$	C=O stretching
1181 $\text{cm}^{-1}$	-	1197 $\text{cm}^{-1}$	Ar <sub>ester</sub> C-O stretching
1019 $\text{cm}^{-1}$	1051 $\text{cm}^{-1}$	1033 $\text{cm}^{-1}$	Alcoholic C-O stretching
-	952 $\text{cm}^{-1}$	949 $\text{cm}^{-1}$	C-N stretching quaternary ammonium salt

Table 3 and Figure 13 show FTIR spectral details for TA-ChCl NADES. As shown in the table 3, a blue shift in the (C=O<sub>v</sub>) stretching frequency from 1699  $\text{cm}^{-1}$  in tannic acid to 1715  $\text{cm}^{-1}$  in TA-ChCl DES. This noticeable shift reveals that carbonyl group of tannic acid is participating in strong hydrogen bonding. There is obvious shifting of

the peaks of alcoholic (C-O  $\nu$ ) stretching in tannic acid and choline chloride from 1019  $\text{cm}^{-1}$  and 1051  $\text{cm}^{-1}$  respectively to 1033  $\text{cm}^{-1}$  in the DES. A minor red shift in (C-N  $\nu$ ) stretching frequency quaternary ammonium salt is noticeable from 952  $\text{cm}^{-1}$  and emerged at 949  $\text{cm}^{-1}$  in TA-ChCl NADES. All these shifting in the vibrational frequencies of tannic acid and choline chloride in DES are attributed to the hydrogen-bonding between tannic acid and choline chloride.

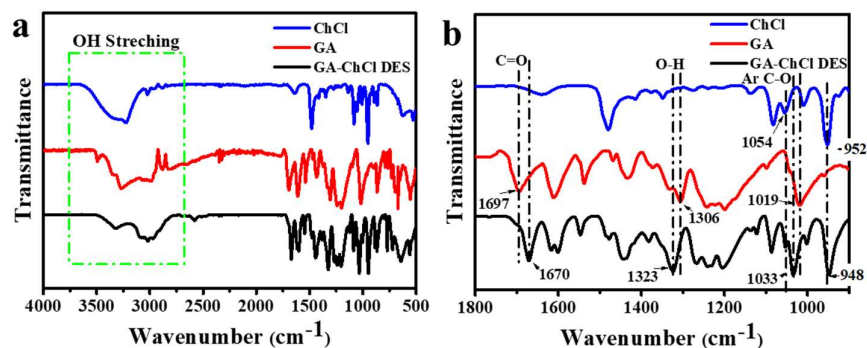


**Figure 14.** a. FTIR spectra of GA-ChCl DES with respect to their components and b. extended FTIR spectra to 1800-600  $\text{cm}^{-1}$  range.

Gallic Acid	Choline Chloride	GA-ChCl DES	Mode
1697 $\text{cm}^{-1}$	-	1670 $\text{cm}^{-1}$	C=O stretching
1306 $\text{cm}^{-1}$	-	1323 $\text{cm}^{-1}$	Phenolic O-H bending
1019 $\text{cm}^{-1}$	1054 $\text{cm}^{-1}$	1033 $\text{cm}^{-1}$	Alcoholic C-O stretching
-	952 $\text{cm}^{-1}$	948 $\text{cm}^{-1}$	C-N stretching quaternary ammonium salt

Table 4 and Figure 14 show FTIR spectral details for GA-ChCl NADES. As shown in the table 3, a red shift in the (C=O  $\nu$ ) stretching frequency from 1697  $\text{cm}^{-1}$  in gallic acid to 1670  $\text{cm}^{-1}$  in GA-ChCl DES. This shift reveals that carbonyl group of gallic acid is

participating in strong hydrogen bonding. There is obvious shifting of the peaks of alcoholic (C-O  $\nu$ ) stretching in gallic acid and choline chloride from 1019  $\text{cm}^{-1}$  and 1054  $\text{cm}^{-1}$  respectively to 1033  $\text{cm}^{-1}$  in the DES. A minor red shift in (C-N  $\nu$ ) stretching frequency quaternary ammonium salt is noticeable from 952  $\text{cm}^{-1}$  and emerged at 948  $\text{cm}^{-1}$  in GA-ChCl NADES. All these shifts in the vibrational frequencies of gallic acid and choline chloride in DES are attributed to the hydrogen-bonding between gallic acid and choline chloride.

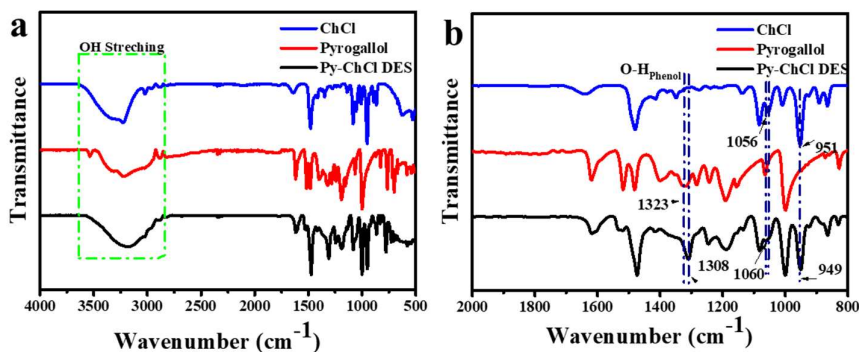


**Figure 15.** a. FTIR spectra of Py-ChCl DES with respect to their components and b. extended FTIR spectra to 1800-600  $\text{cm}^{-1}$  range.

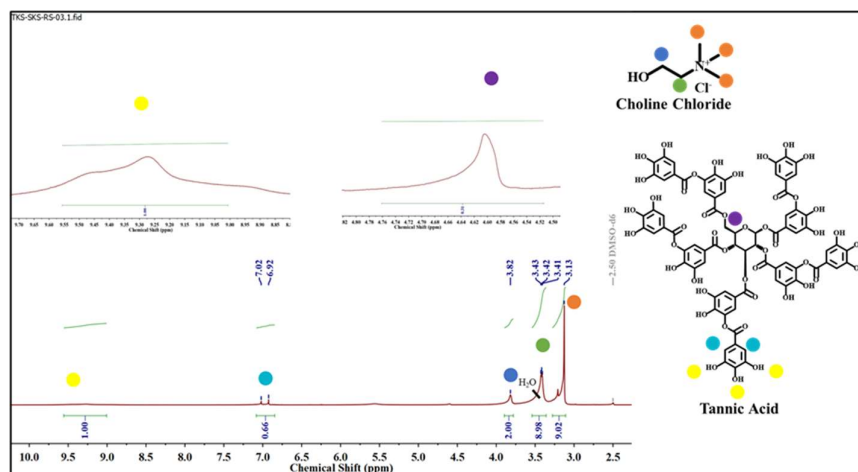
<b>Table 5.</b> Vibrational frequencies of Py-ChCl DES with respect to their components.			
<b>Pyrogallol</b>	<b>Choline Chloride</b>	<b>Py-ChCl DES</b>	<b>Mode</b>
1323 $\text{cm}^{-1}$	-	1306 $\text{cm}^{-1}$	Phenolic O-H bending
-	1056 $\text{cm}^{-1}$	1060 $\text{cm}^{-1}$	Alcoholic C-O stretching
-	951 $\text{cm}^{-1}$	949 $\text{cm}^{-1}$	C-N stretching quaternary ammonium salt

Table 5 and Figure 15 show FTIR spectral evidence for Py-ChCl NADES. From Table 5, a red shift in the (O-H  $\nu$ ) stretching frequency from 1323  $\text{cm}^{-1}$  in pyrogallol to 1306  $\text{cm}^{-1}$  in Py-ChCl DES. This shift suggests that phenolic O-H of pyrogallol is involved in hydrogen bonding. Also, there is a shifting of the peaks of alcoholic (C-O  $\nu$ ) stretching in choline chloride from 1056  $\text{cm}^{-1}$  to 1060  $\text{cm}^{-1}$  in the DES.

A minor shift in (C-N<sub>v</sub>) stretching frequency quaternary ammonium salt is noticeable from 951 cm<sup>-1</sup> and emerged at 949 cm<sup>-1</sup> in Py-ChCl NADES. All these shifts in the vibrational frequencies of pyrogallol and choline chloride in DES are attributed to the hydrogen-bonding between gallic acid and choline chloride.

#### 4.4. <sup>1</sup>H-NMR Spectroscopy

The purity and stability of all three natural polyphenols-based DES was checked using proton NMR spectroscopy. For all choline chloride and HBDs (tannic acid, pyrogallol, gallic acid), proton NMR suggests no chemical changes but broadening and slight shifting of the peak due to the non-covalent interactions among the components of NADES.



**Figure 16.** <sup>1</sup>H-NMR Spectrum of TA-ChCl DES.

In the <sup>1</sup>H-NMR spectrum of the TA-ChCl DES (Figure 16), all the characteristics peaks of the constituents are intact in the NMR spectrum of the DES. Also, any characteristics ester peaks were not observed which suggest that tannic acid and choline chloride binds only through non-covalent interactions.

In the <sup>1</sup>H NMR spectrum of the DES formed from tannic acid and choline chloride (TA-ChCl), all the characteristic peaks corresponding to the individual constituents were present, suggesting that their fundamental structures remained intact. Additionally, no characteristic

ester peaks were observed in the spectrum, indicating that tannic acid and choline chloride bind solely through non-covalent interactions.

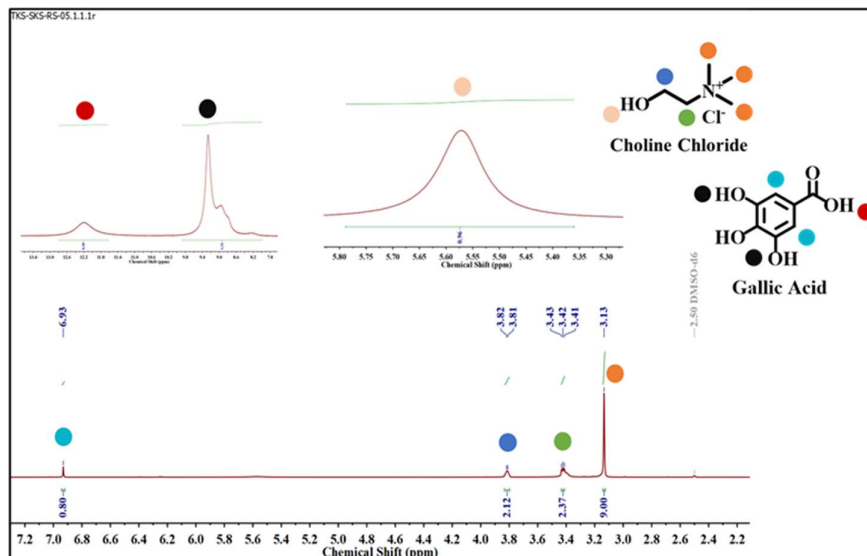


**Figure 17.** <sup>1</sup>H-NMR Spectrum of GA-ChCl DES.

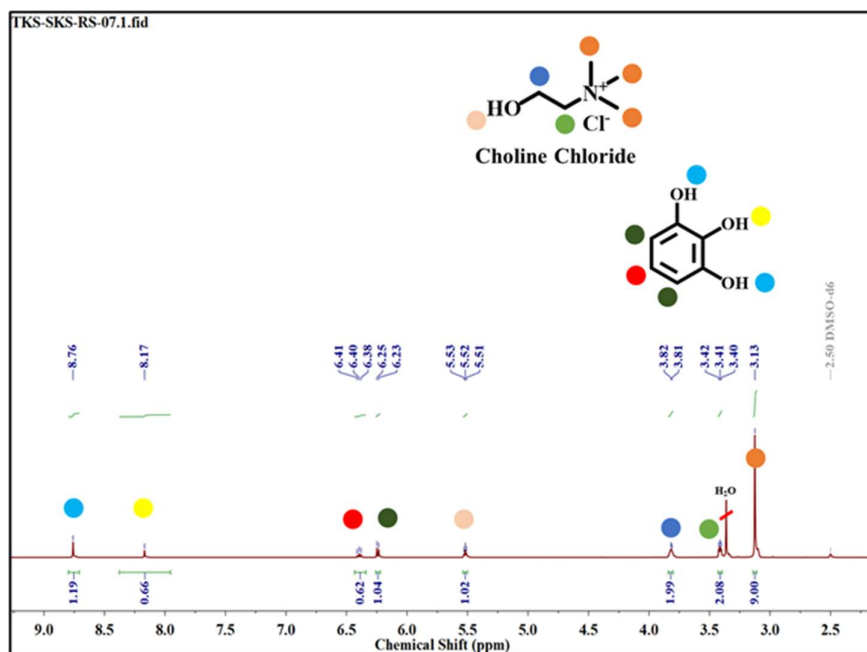


**Figure 18.** <sup>1</sup>H-NMR Spectrum of Py-ChCl DES.

The same analysis can be inferred in the case of GA-ChCl (Figure 17) and Py-ChCl DES (Figure 18).

#### 4.5. Physical properties of prepared NADESs

All three NADESs were prepared with different molar ratios of HBD and HBA. The tannic acid-based NADES is a highly viscous, brown-colored, translucent homogeneous liquid. It was prepared using a 1:20 HBD: HBA molar ratio and demonstrates high solubility in water. The gallic acid-based DES is a transparent, yellowish, viscous liquid formed by combining gallic acid with choline chloride in a 1:3 ratio. The DES containing pyrogallol is a brownish, transparent, viscous liquid. All three polyphenol-based NADESs exhibit a wide range of liquid properties. The physical characteristics of these prepared NADESs are summarized in the [Table 6](#) below:

**Table 6.** Summary of NADESs prepared (physical features).

Hydrogen bond donor	Hydrogen bond acceptor	Molar ratio (HBD:HBA)	Water solubility (mg/mL)	Liquid range temperature (°C)	Aspects
Tannic acid (TA)	Choline Chloride (ChCl)	1:20	2850	20-220	Highly viscous brownish translucent liquid
Gallic acid (GA)		1:3	11.9	35-240	Viscous yellowish transparent liquid
Pyrogallol (Py)		1:2	625	20-220	Viscous brownish transparent liquid

Viscosity is one of the key properties of liquid solvents, as it directly affects their ionic conductivity. Therefore, viscosity is a critical factor in exploring the potential applications of NADESs. The relationship between viscosity and shear rate was measured across a range of shear rates from 0.01 to 10,000 s<sup>-1</sup> at 25 °C.

The viscosity of NADESs is determined by the size and number of functional groups present in the hydrogen bond acceptors (HBAs) and hydrogen bond donors (HBDs). The viscosity tends to increase with the number of functionalities, such as -COOH or -OH groups, in the hydrogen bond donor. This explains why the viscosity of the tannic acid-based DES (TA-ChCl) is higher than that of the pyrogallol-based DES (Py-ChCl).

However, the viscosity versus shear rate for the gallic acid-based NADES could not be measured, as this DES exists as a solid below 35 °C. The size of the hydrogen bond donor can also influence the viscosity of the prepared NADESs, with the larger size of the tannic acid molecule possibly contributing to the higher viscosity observed in the TA-ChCl DES.

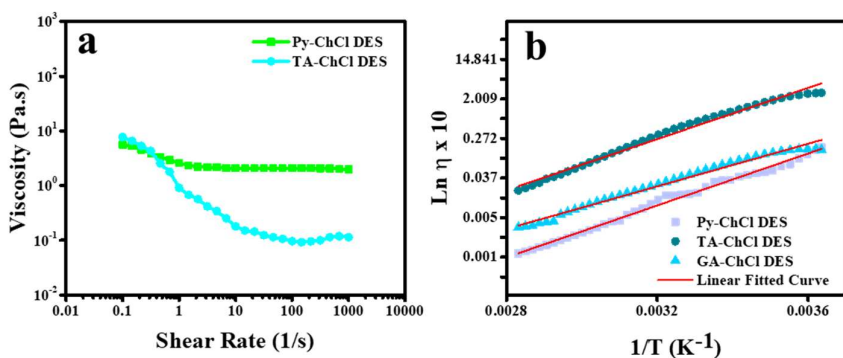


**Figure 19.** a. Viscosity vs. shear rate plot for the Py-ChCl DES and TA-ChCl DES, b. Ln  $\eta$  vs  $1/T$  plots derived from the Arrhenius model.

The viscosities of the NADESs decreases with the increase in the temperature which can be correlated using Arrhenius equation given by:

$$\eta = \eta_0 e^{(E_a/RT)}$$

where  $\eta$  represents the viscosity in Pa s,  $\eta_0$  gives a pre-exponential factor in Pa s,  $E_a$  is the activation energy in J mol<sup>-1</sup>, R the ideal gas constant in (Jmol K)<sup>-1</sup>, and T is the temperature in kelvin (K). The slopes of the logarithmic plots of viscosities of NADESs with  $1/T(K^{-1})$

tells us about their activation energy of the ionic movements in the NADES which can reveal about the extent of interactions among the components of the resulting NADES (Figure 19b, Table 7).

<b>Table 7. E<sub>a</sub> values as a function of temperature.</b>		
NADES	E <sub>a</sub> (Jmol <sup>-1</sup> )	R <sup>2</sup>
TA-ChCl	776	0.9874
GA-ChCl	646.89	0.9855
Py-ChCl	787.93	0.9937

The trend for activation energy of different prepared NADES can be represented as follows:



This trend suggests that the gallic acid-based DES (GA-ChCl), having a lower activation energy, may exhibit better solubilizing capacity for metal oxides compared to the other DESs. Thus, we can conduct a temperature dependent leaching study for insoluble metal oxides using the prepared DESs aiding us in achieving the most effective leaching medium.

#### **4.6. Dissolution of metal ions into Prepared NADES**

The dissolution of metal ions is influenced by several factors, including leaching temperature, the type of hydrogen bond donors (HBDs) used in NADESs, and the duration of the leaching process. In a typical experiment, 20 mg of LCO powder was added to 1 g of the prepared DES, and this mixture was leached at temperatures ranging from 80 °C to 160 °C for a fixed duration of 12 hours.

Although color changes can indicate the solubilization of metal salts in DESs, the inherently dark color of these NADESs made it difficult to visually detect any changes as the temperature varied. Consequently, metal dissolution was quantified using Inductively Coupled Plasma Atomic Emission Spectroscopy (ICPAES). The ICPAES results

showed that the concentration of dissolved metals increased as the temperature rose from 80 °C to 140 °C. Among the DESs tested, the gallic acid-based DES (GA-ChCl) exhibited the best performance, yielding the highest concentrations of dissolved cobalt and lithium (Figure 20). This result implies with the activation energy calculations of the DESs, inferring that the less activation energy is improving the metal solubility using the DESs.

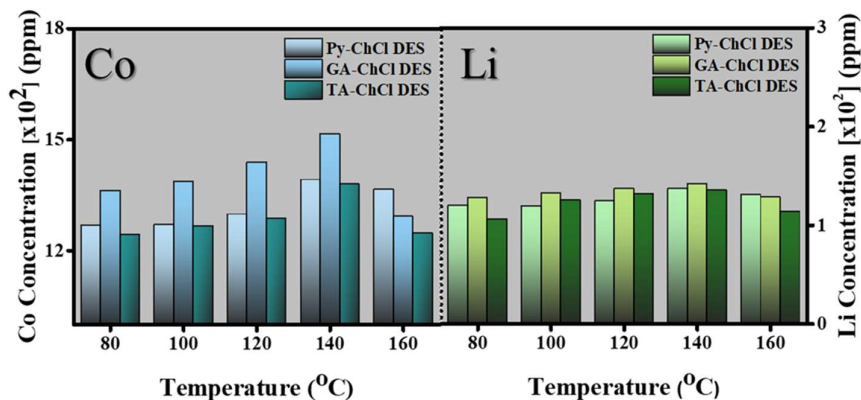


**Figure 20.** Leaching efficiencies of Py-ChCl DES, GA-ChCl DES and Ta-ChCl DES towards Lithium cobalt oxide (LCO) powder at variable temperature scale.

Based on the Figure 20, the metal extraction efficiencies for all three prepared NADESs increased as the temperature rose, reaching a peak at 140 °C. However, a slight decline in efficiency was observed when the temperature reached 160 °C. Therefore, 140 °C appears to be the optimal temperature for leaching treatment within the given range.

#### 4.6.1. Solubilization of LCO powder as a model compound for leaching treatment at variable timescale

After optimizing the leaching temperature, the solubility of LCO powder was analyzed over a 24-hour period, with measurements taken at intervals of 1, 2, 4, 8, 12, 18, and 24 hours at a constant temperature of 140 °C. The filtered leachates were then subjected to quantitative analysis using Inductively Coupled Plasma Atomic Emission

Spectroscopy (ICPAES) to determine the leaching efficiency of the prepared NADESs. The results, which indicated the leaching efficiency of various metals for each NADES, were plotted against time (in hours).

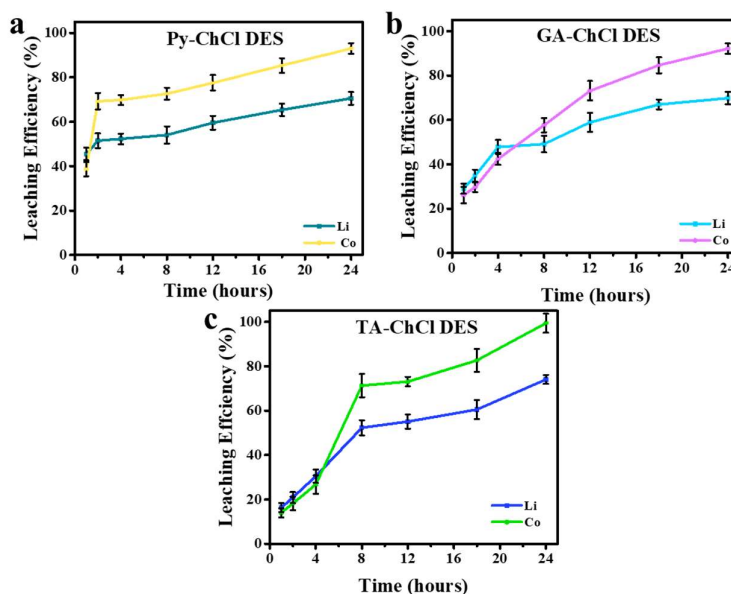


**Figure 21.** Extraction of lithium and cobalt from LCO powder using **a.** Py-ChCl DES, **b.** GA-ChCl DES and **c.** TA-ChCl DES at variable time scale.

From [Figure 21](#), the amount of extracted metal ions increases with time, reaching its peak at 24 hours. The Py-ChCl NADES showed high recovery rates for cobalt and lithium, with extraction efficiencies of 93% for cobalt and over 70% for lithium. The extraction rate for cobalt exhibited a rapid rise in the first few hours, doubling within 2 hours.

The GA-ChCl DES also demonstrated strong leaching efficiency, with extraction rates of 92% for cobalt and 70% for lithium at 24 hours. In the case of TA-ChCl NADES, the amount of leached cobalt almost tripled between 4 and 8 hours, increasing from 26.7% to 71.3%. Ultimately, TA-ChCl NADES achieved a remarkable extraction rate of 99.4% for cobalt from LCO powder at 24 hours of leaching.

Overall, the leaching efficiencies for both lithium and cobalt were found to be highest at the 24-hour mark for all three NADESs. This indicates that a longer extraction time leads to more effective recovery of these metal ions.

#### **4.6.2. Solubilization of spent Li-ion battery (LIB) powder for leaching treatment**

The increasing use of lithium-ion batteries in electric vehicles and the high demand for mobile devices have led to a significant accumulation of waste lithium-ion batteries, therefore leading to a need for green recycling methods. In this context, optimized leaching experiments were conducted to extract valuable metals like cobalt, lithium, nickel, and manganese from end-of-life battery cathode materials. These metals are crucial to produce new batteries and other high-tech applications, making their recovery from spent batteries not only environmentally beneficial but also economically advantageous.

From [Figure 22](#), it is evident that lithium is the most leached metal ion, while nickel is the least leached among all the metal ions. These soluble metal ions from the lithium cobalt oxide (LCO) and lithium-ion battery (LIB) leachates can be separated by converting them into insoluble precipitates through a chemical precipitation method.

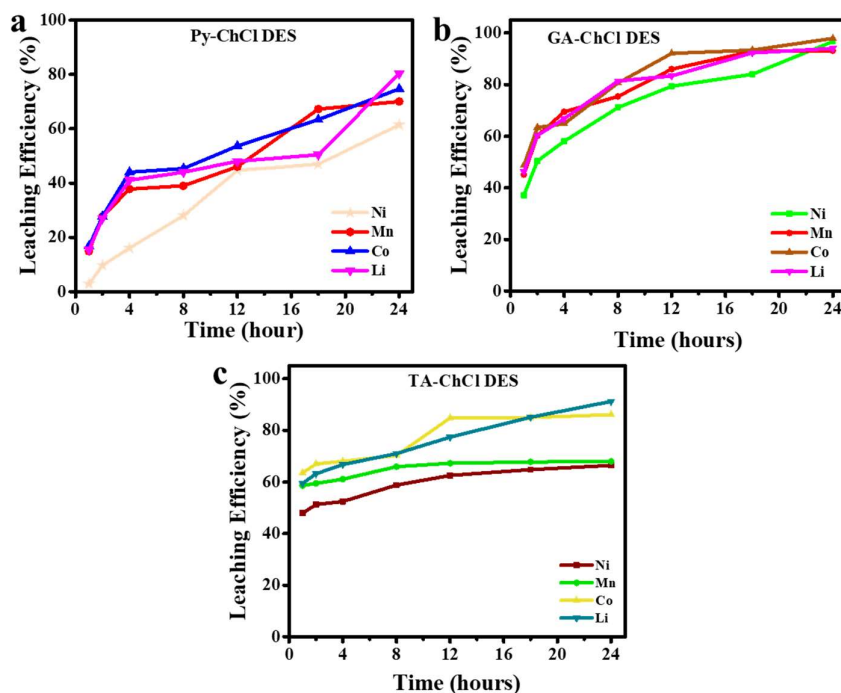


**Figure 22.** Extraction of valuable metals from spent lithium-ion batteries using **a.** Py-ChCl DES, **b.** GA-ChCl DES, **c.** TA-ChCl DES as a leaching agent.

#### 4.7. Leaching Mechanism

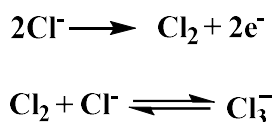
Understanding the mechanism of the leaching process is crucial for gaining deeper insights into how it works. Abbott et al. highlighted the importance of oxygen acceptors in DES for dissolving metal oxides. In the case of cobalt dissolution in NADES, a color change was observed, transitioning from the solvent's original color to green during leaching, and eventually to dark brown<sup>35,36</sup>.

UV-visible spectroscopic studies on the leachate showed three distinct peaks near 630 nm, 668 nm, and 698 nm, indicating the formation of a tetrahedral cobalt complex. Given the high concentration of Cl<sup>-</sup> ions in the solvent, this tetrahedral complex is likely to be [CoCl<sub>4</sub>]<sup>2-</sup>, which aligns with the observed UV-visible spectrum.

The complete leaching process can be broken down into 2 crucial steps<sup>38</sup>:

## 1. Formation of $\text{Cl}_3^-$ ion as oxidizing agent

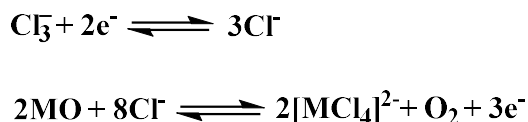
The first step of leaching process involves the oxidation of  $\text{Cl}^-$  ion of choline chloride to  $\text{Cl}_2$  followed by the formation of  $\text{Cl}_3^-$  ions as per the equation mentioned below:



This  $\text{Cl}_3^-$  ion acts as oxidizing agent and the metal in metal oxide gets reduced from  $\text{M}^{3+}$  to  $\text{M}^{2+}$  ion.

## 2. Formation of chlorometallates

The metal oxide reacts in-situ with chloride ions present in solvent media to form soluble chlorometallates. This step can be precisely represented by the given reaction:



## 4.8. Metal Recovery from selective precipitation method

The dissolved metal ions in the leachates from treated lithium cobalt oxide (LCO) and lithium-ion batteries (LIB) were recovered using a chemical precipitation method for LCO and a multistage chemical precipitation method for LIB, following the approach of Qi Meng et al. The resulting precipitates were analyzed using Scanning Electron Microscopy with Energy Dispersive Spectroscopy (SEM-EDS) to gain insights into the characteristics of the precipitation products.

In the case of the LCO leachate, the precipitated cobalt product appeared as a black-colored powder, as shown in the inset. SEM-EDS images were used to examine the precipitation products before and after calcination, providing valuable information on their morphology and elemental composition. This analysis allows researchers to

evaluate the quality and structure of the precipitates, as well as to identify potential impurities or changes resulting from calcination.

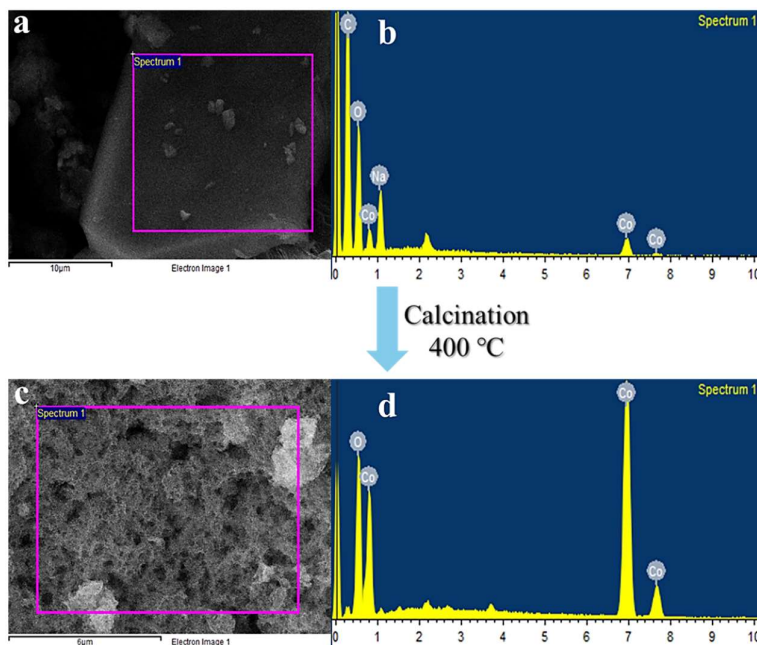


**Figure 23.** SEM-EDS images of recovered Cobalt (a,b)  $\text{CoCO}_3$  (c,d)  $\text{Co}_3\text{O}_4$  form LCO leachate.

Figure 23a represents morphology of the initial product after chemical precipitation as cobalt carbonate,  $\text{CoCO}_3$  with the EDX graph inferring the formation of cobalt carbonate. Again, after calcination of the  $\text{CaCO}_3$  salts a homogeneous  $\text{Co}_3\text{O}_4$  formed which can be shown by the morphology (Figure 23c) and the EDX graphs (Figure 23d).

In this study, we employed a multi-step directional precipitation strategy to recover metals from the leachates of spent lithium-ion battery (LIB) cathode material. After the leachates from the LIB powder treated with DESs were collected, they were filtered through nylon filters to remove polymers and carbon black residues. The selective precipitation process was then used to separate manganese (Mn), nickel (Ni), and cobalt (Co) in a step-by-step manner<sup>37</sup>.

Due to the lower abundance and reactivity of lithium (Li) in the LIB powders, it was not possible to selectively precipitate the Li ions.

Although selective precipitation is a well-established technique, its application for recovering metal ions from leachates obtained via DES leaching is relatively underexplored.

The precipitates of LIB leachate were analyzed using SEM-EDS images. Dissolved  $\text{Mn}^{2+}$  ions were precipitated into black colored mixture of  $\text{MnO}_2$  and  $\text{Mn}_2\text{O}_3$  (Figure 24 a,b) (inset). The EDS map also agrees with the components of mixture of metal oxide.

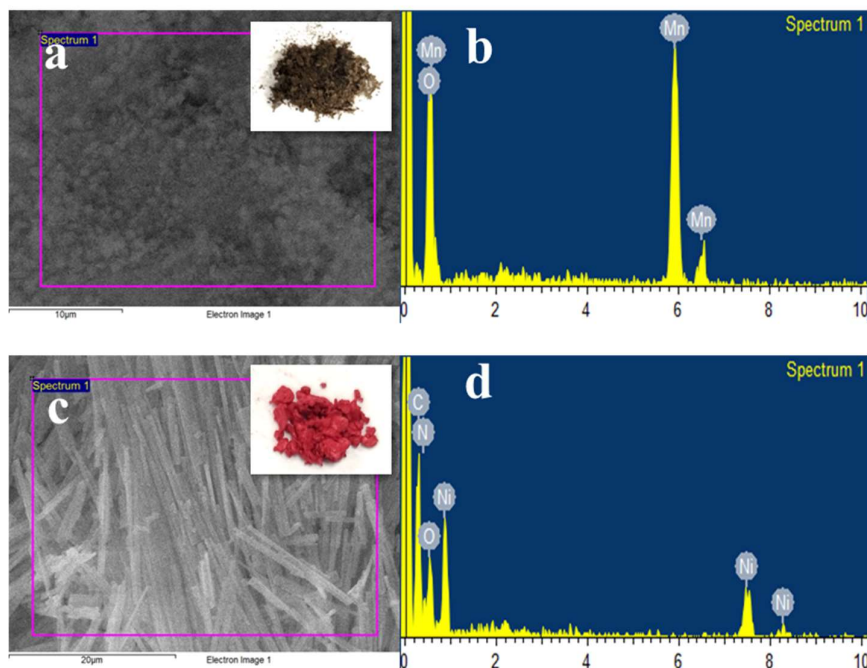


**Figure 24.** SEM-EDS images of recovered Mn (a,b), Ni (c,d) from spent LIB powder.

The  $\text{Ni}^{2+}$  ions were precipitated into a cherry red colored water insoluble  $\text{Ni}(\text{DMG})_2$  as shown in SEM EDS images and EDX graphs (Figure 24 c,d).

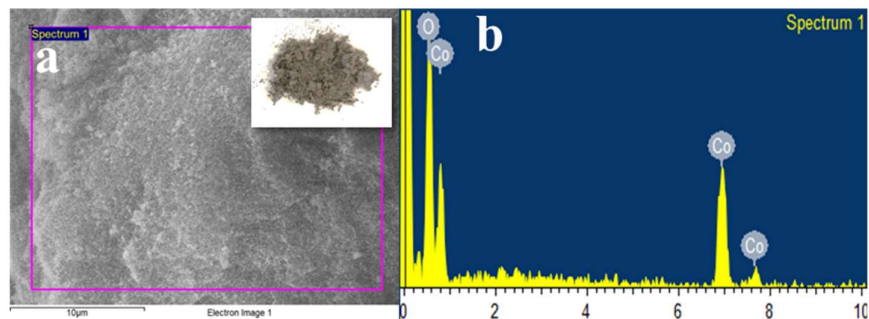


**Figure 25.** SEM-EDS images of recovered cobalt (**a,b**) from spent LIB powder.

The  $\text{Co}^{2+}$  ions were precipitated into a pink colored water insoluble  $\text{Co}(\text{OH})_2$  as shown in SEM image and EDX graph (Figure 25).

## 5. Chapter 5

### Conclusion

Natural Deep eutectic solvents are an emerging class of green solvent due to their less hazardous properties to health and environment. These DESs constitute hydrogen-bond acceptors and hydrogen bond donors which participate in hydrogen-bonding to give DESs. Report reveals that Type 3 DES can be useful for spent Li-ion batteries treatment with high recovery rate of metals from spent LIBs.

In this report, we have prepared three DES namely TA-ChCl, GA-ChCl and Py-ChCl using choline chloride as hydrogen bond acceptor and tannic acid, gallic acid and pyrogallol as hydrogen bond donors respectively. The stability and purity of NADESs was assessed by proton NMR spectroscopy, UV-spectroscopy and FT-IR spectroscopy are found to be stable at room temperature. The gallic acid-based NADES is transparent, low viscous yellowish liquid above 35 °C. Pyrogallol and tannic acid-based NADESs are dark brown viscous liquid at room temperature. The viscosity has been evaluated and activation energies of the DESs are calculated by correlating with Arrhenius equation.

The prepared Deep Eutectic Solvents (DESs) were used as a potential leaching medium for the extraction of lithium cobalt oxide, a model cathode material, as well as spent lithium-ion battery cathode powder, aiming to recover valuable metals such as cobalt, lithium, nickel, and manganese. All the DESs demonstrated a potential ability to leach the battery waste powder, but among them, the gallic acid-based DES outperformed the others due to its lower activation energy, leading to greater solubility of metal oxides.

A unique method for selectively precipitating metal ions from the leachate has been implemented, allowing cobalt, nickel, and manganese to be efficiently extracted with high selectivity. The

precipitated metal salts were then analyzed for their morphology and chemical composition using energy-dispersive X-ray spectroscopy.

### **Future Scopes of the Work Plan**

The presence of tea-derived polyphenols in DESs makes it a potential candidate for leaching applications for the end-of-life Li-ion battery. The leaching treatment using NADESs can be applied to the extraction of metal ions from the mixture of metal salts and various precious metals such as gold, platinum etc. present in e-waste. The DESs reported for recycling process so far, contains choline chloride as its hydrogen-bond acceptor. There are many other possible moieties such as phosphonium ions which can act as hydrogen-bond acceptors. The selection of appropriate hydrogen-bond donor and acceptor can also lead to appreciable results. With the help of computational modelling, the eutectic parameters for desirous properties can be calculated precisely for the target DES as per the applications in [section 1.3](#).

Designing an appropriate catalytic moiety can also boost the metal extraction process from different chemistries.

## 6. Chapter 6

### References

1. Hansen, B. B., Spittle, S., Chen, B., Poe, D., Zhang, Y., Klein, J. M., Horton, A., Adhikari, L., Zelovich, T., Doherty, B. W., Gurkan, B., Maginn, E. J., Ragauskas, A., Dadmun, M., Zawodzinski, T. A., Baker, G. A., Tuckerman, M. E., Savinell, R. F., Sangoro, J. R. (2021), Deep Eutectic Solvents: A Review of Fundamentals and Applications, *Chem. Rev.*, 121, 1232–1285 (DOI: 10.1021/acs.chemrev.0c00385)
2. Worsfold Paul, Alan Townshend, Colin F. Poole, and Manuel Miró, (2019), *Encyclopedia of analytical science*. Elsevier, (ISBN: 978-0-08-101983-2)
3. Picchio, M. L., Minudri, D., Mantione, D., Criado-Gonzalez, M., Guzmán-González, G., Schmarsow, R., Müller, A. J., Tomé, L. C., Minari, R. J., Mecerreyes, D. (2022), Natural Deep Eutectic Solvents Based on Choline Chloride and Phenolic Compounds as Efficient Bioadhesives and Corrosion Protectors, *ACS Sustain. Chem. Eng.*, 10, 8135–8142 (DOI: 10.1021/acssuschemeng.2c01976)
4. Wang, S., Zhang, Z., Lu, Z., Xu, Z. (2020), A Novel Method for Screening Deep Eutectic Solvent to Recycle the Cathode of Li-Ion Batteries, *Green Chem.*, 22, 4473–4482 (DOI: 10.1039/D0GC00701C)
5. Tomé, L. I. N., Baião, V., da Silva, W., Brett, C. M. A. (2018), Deep Eutectic Solvents for the Production and Application of New Materials, *Appl. Mater. Today.*, 10, 30–50 (DOI: 10.1016/j.apmt.2017.11.005)
6. Dai, Y., van Spronsen, J., Witkamp, G.J., Verpoorte, R., Choi, Y. H. (2013), Natural Deep Eutectic Solvents as New Potential Media for Green Technology, *Anal. Chim. Acta*, 766, 61–68 (DOI: 10.1016/j.aca.2012.12.019)

7. Abbott, A. P., Barron, J. C., Ryder, K. S., Wilson, D. (2007), Eutectic based Ionic Liquids with Metal-containing Anions and Cations, *Chem. Eur. J.*, 13, 6495–6501 (DOI:10.1002/chem.200601738)
8. Abranches, D. O., Martins, M. A., Silva, L. P., Schaeffer, N., Pinho, S. P., Coutinho, J. A. (2019), Phenolic Hydrogen Bond Donors in the Formation of Non-ionic Deep Eutectic Solvents: The Quest for Type V DES, *Chem. Commun.*, 55, 10253–10256 (DOI: 10.1039/C9CC04846D)
9. Blusztajn, J. K. (1998), Choline, a Vital Amine, *Science*, 281, 794–795 (DOI: 10.1126/science.281.5378.794)
10. Abbott, A. P., Boothby, D., Capper, G., Davies, D. L., Rasheed, R. K. (2004), Deep Eutectic Solvents Formed Between Choline Chloride and Carboxylic Acids: Versatile Alternatives to Ionic Liquids, *J. Am. Chem. Soc.*, 126, 9142–9147 (DOI: 10.1021/ja048266j)
11. Soldner, A., Zach, J., König, B. (2019), Deep Eutectic Solvents as Extraction Media for Metal Salts and Oxides Exemplarily Shown for Phosphates from Incinerated Sewage Sludge Ash, *Green Chem.*, 21, 321–328 (DOI: 10.1039/C8GC02702A)
12. Migliorati, V., Sessa, F., D'Angelo, P. (2019), Deep Eutectic Solvents: A Structural Point of View on the Role of the Cation, *Chem. Phys. Lett.*: X, 2, 100001 (DOI: 10.1016/j.cpletx.2018.100001)
13. Gomez, E., Cojocar, P., Magagnin, L., Valles, E. (2011), Electrodeposition of Co, Sm and SmCo from a Deep Eutectic Solvent, *J. Electroanal. Chem.*, 658, 18–24 (DOI: 10.1016/j.jelechem.2011.04.015)
14. Abbott, A. P., Capper, G., McKenzie, K. J., Ryder, K. S. (2007), Electrodeposition of Zinc-tin Alloys from Deep Eutectic Solvents Based on Choline Chloride, *J. Electroanal. Chem.*, 599, 288–294 (DOI: 10.1016/j.jelechem.2006.04.024)

15. Abbott, A. P., McKenzie, K. J., Ryder, K. S. (2007), Electropolishing and Electroplating of Metals Using Ionic Liquids Based on Choline Chloride, 975, 186–197 (DOI: 10.1021/bk-2007-0975.ch013)
16. Zhu, A., Jiang, T., Han, B., Zhang, J., Xie, Y., Ma, X. (2007), Supported Choline Chloride/urea as a Heterogeneous Catalyst for Chemical Fixation of Carbon Dioxide to Cyclic Carbonates, *Green Chem.*, 9, 169–172 (DOI: 10.1039/B612164K)
17. Zein El Abedin, S., Endres, F. (2007), Ionic Liquids: The Link to High-Temperature Molten Salts?, *Acc. Chem. Res.*, 40, 1106– 1113 (DOI: 10.1021/ar700049w)
18. Jiang, Z. M., Wang, L. J., Gao, Z., Zhuang, B., Yin, Q., Liu, E. H. (2019), Green and Efficient Extraction of Different Types of Bioactive Alkaloids Using Deep Eutectic Solvents, *Microchem. J.*, 145, 345–353 (DOI: 10.1016/j.microc.2018.10.057 )
19. Akinosho, H., Rydzak, T., Borole, A., Ragauskas, A., Close, D. (2015), Toxicological Challenges to Microbial Bioethanol Production and Strategies for Improved Tolerance, *Ecotoxicology*, 24, 2156– 2174 (DOI: 10.1007/s10646-015-1543-4)
20. Agrawal, R., Verma, A., Satlewal, A. (2016), Application of Nanoparticle-immobilized Thermostable B-glucosidase for Improving the Sugarcane Juice Properties, *Innovative Food Sci. Emerging Technol.*, 33, 472–482 (DOI: 10.1016/j.ifset.2015.11.024)
21. Xia, S., Baker, G. A., Li, H., Ravula, S., Zhao, H. (2014), Aqueous Ionic Liquids and Deep Eutectic Solvents for Cellulosic Biomass Pretreatment and Saccharification, *RSC Adv.*, 4, 10586–10596 (DOI: 10.1039/C3RA46149A)
22. Satlewal, A., Agrawal, R., Bhagia, S., Sangoro, J., Ragauskas, A. J. (2018), Natural Deep Eutectic Solvents for Lignocellulosic Biomass Pretreatment: Recent Developments,

- Challenges and Novel Opportunities, *Biotechnol. Adv.*, 36, 2032 (DOI: 10.1016/j.biotechadv.2018.08.009)
23. Mbous, Y. P., Hayyan, M., Hayyan, A., Wong, W. F., Hashim, M. A., Looi, C. Y. (2017), Applications of Deep Eutectic Solvents in Biotechnology and Bioengineering-promises and Challenges, *Biotechnol. Adv.* 35, 105–134 (DOI: 10.1016/j.biotechadv.2016.11.006)
24. Vigier, K. D. O., Chatel, G., Jérôme, F. (2015), Contribution of Deep Eutectic Solvents for Biomass Processing: Opportunities, Challenges, and Limitations, *ChemCatChem*, 7, 1250–1260 (DOI: 10.1002/cctc.201500134)
25. Loow, Y.-L., Wu, T. Y., Yang, G. H., Ang, L. Y., New, E. K., Siow, L. F., Jahim, J. M., Mohammad, A. W., Teoh, W. H. (2018), Deep Eutectic Solvent and Inorganic Salt Pretreatment of Lignocellulosic Biomass for Improving Xylose Recovery, *Bioresour. Technol.*, 249, 818–825 (DOI: 10.1016/j.biortech.2017.07.165)
26. Morrison, H. G., Sun, C. C., Neervannan, S. (2009), Characterization of Thermal Behavior of Deep Eutectic Solvents and Their Potential as Drug Solubilization Vehicles, *Int. J. Pharm.*, 378, 136–139 (DOI: 10.1016/j.ijpharm.2009.05.039)
27. Shirani, M., Habibollahi, S., Akbari, A. (2019), Centrifuge-less Deep Eutectic Solvent Based Magnetic Nanofluid-linked Air-agitated Liquid-liquid Microextraction Coupled with Electrothermal Atomic Absorption Spectrometry for Simultaneous Determination of Cadmium, Lead, Copper, and Arsenic in Food Samples and Nonalcoholic Beverages, *Food Chem.*, 304–311 (DOI: 10.1016/j.foodchem.2018.12.110)
28. Pradeepkumar, P., Elgorban, A., Bahkali, A., Rajan, M. (2018), Natural Solvent-assisted Synthesis of Amphiphilic Copolymeric Nanomicelles for Prolonged Release of

- Camptothecin Delivery, *New J. Chem.*, 42, 10366–10375 (DOI: 10.1039/C8NJ00901E)
29. Buckley, M. M., Benfield, P. (1993), Eutectic Lidocaine/Prilocaine Cream, *Drugs*, 46, 126–151 (DOI: 10.2165/00003495-199346010-00008)
30. Griffin, P. J., Cosby, T., Holt, A. P., Benson, R. S.; Sangoro, J. R. (2014), Charge Transport and Structural Dynamics in Carboxylic acid-based Deep Eutectic Mixtures, *J. Phys. Chem. B*, 118, 9378–9385 (DOI: 10.1021/jp503105g)
31. Xing, L., Zhang, H., Qi, R., Tsao, R., Mine, Y. (2019), Recent Advances in the Understanding of the Health Benefits and Molecular Mechanisms Associated with Green Tea Polyphenols. *J. Agric. Food Chem.*, 67, 1029–1043 (DOI: 10.1021/acs.jafc.8b06146)
32. Tran, M. K., Rodrigues, M., Kato, K., Babu, G., Ajayan, P. M. (2019), Deep eutectic solvents for cathode recycling of Li-ion batteries, *Nature Energy*, 4(4), 339-345 (DOI: 10.1038/s41560-019-0368-4)
33. Abbott, A. P., Capper, G., Davies, D. L., Rasheed, R. K., Tambyrajah, V. (2003), Novel Solvent Properties of Choline Chloride Urea Mixture, *Chem. Commun.*, 0, 70–71 (DOI: 10.1039/B210714G)
34. Chen, L., Chao, Y., Li, X., Zhou, G., Lu, Q., Hua, M., Li, H., Ni, X., Wu, P., Zhu, W. (2021) Engineering a tandem leaching system for the highly selective recycling of valuable metals from spent Li-ion batteries, *Green Chem.*, 23, 2177-2184 (DOI: 10.1039/D0GC03820B)
35. Padwal, C., Pham, H. D., Jadhav, S., Do, T. T., Nerkar, J., My Hoang, L. T., Nanjundan, A. K., Mundree, S. G., Dubal, D. P. (2022), Deep Eutectic Solvents: Green Approach for Cathode Recycling of Li-Ion Batteries, *Adv. Energy Sustainability Res.*, 3, 2100133 (DOI: 10.1002/aesr.202100133)

36. Wang, S., Zhang, Z., Lu, Z., Xu, Z. (2020), A novel method for screening deep eutectic solvent to recycle the cathode of Li-ion batteries. *Green Chem.*,22, 4473-4482 (DOI: 10.1039/D0GC00701C)
37. Yang, X., Zhang, Y., Meng, Q., Dong, P., Ning, P., Li, Q. (2021), Recovery of valuable metals from spent lithium-ion batteries by multi-step directional precipitation. *RSC Adv.*, 11, 268-277 (DOI: 10.1039/D0RA09297E)
38. Schiavi, P. G., Altimari, P., Saturabotti, E., Marrani, A.G., Simonetii, Pagnanelli, F. (2022), Decomposition of deep eutectic solvent aids metals extraction in lithium-ion batteries recycling, *ChemSusChem*, 15, e202200966 (DOI: 10.1002/cssc.202200966)

